

JAERI-M

7724

EFFECT OF DIFFERENCE BETWEEN GROUP
CONSTANTS PROCESSED BY CODES TMS
AND ETOX ON INTEGRAL QUANTITIES

June 1978

Hideki TAKANO, Yasushi MATSUI* and Yukio ISHIGURO

この報告書は、日本原子力研究所が JAERI-M レポートとして、不定期に刊行している研究報告書です。入手、複製などのお問い合わせは、日本原子力研究所技術情報部（茨城県那珂郡東海村）あて、お申しこしください。

JAERI-M reports, issued irregularly, describe the results of research works carried out in JAERI. Inquiries about the availability of reports and their reproduction should be addressed to Division of Technical Information, Japan Atomic Energy Research Institute, Tokai-mura, Naka-gun, Ibaraki-ken, Japan.

Effect of Difference between Group Constants
Processed by Codes TIMS and ETOX on Integral Quantities

Hideki TAKANO, Yasushi MATSUI* and Yukio ISHIGURO

Division of Reactor Engineering, Tokai Research Establishment, JAERI

(Received May 25, 1978)

Group constants of ^{235}U , ^{238}U , ^{239}Pu , ^{240}Pu and ^{241}Pu have been produced with the processing code TIMS using the evaluated nuclear data of JENDL-1. The temperature and composition dependent self-shielding factors have been calculated for the two cases with and without considering mutual interference resonant nuclei.

By using the group constants set produced by the TIMS code, the integral quantities, i.e. multiplication factor, Na-void reactivity effect and Doppler reactivity effect, are calculated and compared with those calculated with the use of the cross sections set produced by the ETOX code to evaluate accuracy of the approximate calculation method in ETOX. There is much difference in self-shielding factor in each energy group between the two codes. For the fast reactor assemblies under study, however, the integral quantities calculated with these two sets are in good agreement with each other, because of eventual cancelation of errors.

Keywords ; Group Constant Sets, Uranium, Plutonium, ETOX Code, TIMS Code,
Accuracy of Calculation Method, JENDL-1 Nuclear Data, Self-shielding
Factors, Multiplication Factor, Doppler Effect, Na-void Effect.

プロセスコードTIMSとETOXで計算した炉定数間の差の積分量への影響

日本原子力研究所東海研究所原子炉工学部

高野 秀機・松井 泰・石黒 幸雄

(1978年5月25日受理)

^{235}U , ^{238}U , ^{239}Pu , ^{240}Pu と ^{241}Pu の群定数を評価済み核データ JENDL-1 を用いて、プロセスコードTIMSでもって作成した。その際温度と組成依存の自己遮蔽因子を、異核種間の干渉効果を考慮した場合と考慮しない場合について計算した。

一方、ETOXコードで用いられている近似計算法の精度を評価するために、TIMSとETOXで作成した群定数を用いて積分量；実効増倍係数、ナトリウム・ボイド及びドップラー反応効果を計算し、それらの結果を比較した。自己遮蔽因子間にはかなりの差が各エネルギー群で見られるが、ここで考えられた高速臨界集合体については、これら2つのセットで計算された積分量は互いに良く一致している。この一致は誤差の偶然的な打ち消し合いのためである。

* 日本情報サービス(株)

Contents

1. Introduction	1
2. Production Method for Group Constants of Heavy Resonant Nuclei in Resonance Energy Region	3
3. Comparison of Integral Quantities Calculated by Two Group Cross Section Sets Obtained from TIMS and ETOX Methods	8
4. Concluding Remarks	12
Acknowledgments	13
References	14
Appendix : Tables of 70 Group Constants of ^{235}U , ^{238}U , ^{239}Pu , ^{240}Pu and ^{241}Pu Produced by the Processing Code TIMS Using the Evaluated Nuclear Data of JENDL-1	44

目 次

1. 序 論	1
2. 共鳴領域における重い共鳴核種の群定数の作成方法	3
3. TIMSとETOXの方法で作成した2つの群定数セットから計算された 積分量の比較	8
4. 結 論	12
謝 辞	13
参考文献	14
附 録 : JENDL-1 核データからTIMSコードでもって作成した ^{235}U , ^{238}U , ^{239}Pu , ^{240}Pu と ^{241}Pu の 70 群定数表	44

1. Introduction

Nuclear design calculations and analyses of experiments of fast reactors are usually performed by the use of multigroup transport or diffusion theory codes. The multigroup calculations are often based on the concept of multigroup constants set such as the ABBN⁽¹⁾ or JAERI-Fast set.⁽²⁾⁽³⁾⁽⁴⁾ The principal advantage of multigroup constant method is that the calculation of integral quantities can be made by using the same set of multigroup constants for the various reactors with different compositions and sizes. Consequently, there has been arisen a need to develop a computer code which economically and conveniently calculates these group constants using an updated nuclear data file. For this purpose, some processing codes such as SUPERTOG,⁽⁵⁾ PROF-GROUCH-G,⁽⁶⁾ PROF-GROUCH-G-II,⁽⁷⁾ ETOX⁽⁸⁾ and TIMS,⁽⁹⁾ were developed. However, calculational methods of group constants used in these codes are different. Especially, the effective cross sections in resonance energy region are calculated by using various methods. The difference of these methods affects the final results of integral quantities in neutronics calculation of fast reactors. It is essential in reactor calculation to well comprehend the effect of these different methods on integral quantities.

In the present report, we study the influence of two different group cross sections sets on some integral quantities: One was produced^(*) by using the processing codes PROF-GROUCH-G-II and ETOX, and another was produced by PROF-GROUCH-G-II and TIMS. The evaluated nuclear data of JENDL-1⁽¹⁰⁾ were used in these calculations. The codes ETOX and TIMS calculate the group cross sections of heavy resonant nuclides in the

(*) The calculation of group constants was performed by the Reactor Group Constants Working Group of JNDC.

resonance energy regions. In the two sets, the group constants of light and medium nuclei and of heavy nuclei in smooth region above resonance energy have been calculated by the PROF-GROUCH-G-II code. Thus, the effects of different methods between TIMS and ETOX on integral quantities can be studied by performing the neutronics calculation using two group constants sets.

In the ETOX code, the effective group cross sections are calculated by assuming the constancy of collision density. Moreover, the isolated narrow resonance approximation is used in the unresolved resonance region. On the other hand, in order to avoid the calculational errors⁽¹¹⁾ caused from these approximations, the TIMS code calculates the effective cross sections by directly solving the neutron slowing down equation using the recurrence formula for slowing down source. For this purpose, the TIMS code generates a ladder of resonance levels and parameters by using Monte Carlo method in the unresolved resonance region.

The difference between TIMS and ETOX methods are described in detail and the self-shielding factors calculated with two codes are compared in Chapter 2. Some integral quantities, such as effective multiplication factors and Doppler reactivity worths were calculated by using these different group constants sets, and compared with the experimental results. The comparisons of these results are given in Chapter 3.

The group constants of five nuclides, ^{235}U , ^{238}U , ^{239}Pu , ^{240}Pu and ^{241}Pu calculated by the TIMS code are shown in Appendix.

2. Production Method for Group Constants of Heavy Resonant Nuclei in Resonance Energy Region

The effective group cross sections are defined by the following equation:

$$\tilde{\sigma}_{x,i} = \frac{\int_{\Delta E_i} \sigma_x(E,T)\phi(E)dE}{\int_{\Delta E_i} \phi(E)dE}, \quad (1)$$

where $\sigma_x(E,T)$ is an energy and temperature dependent resonance cross section, the subscript x stands for capture, fission and elastic scattering reactions, ΔE_i the energy width of the considered group i and $\phi(E)$ the neutron flux. In the conventional method, the calculation of Eq.(1) is usually performed by assuming the constant collision density, that is,

$$\phi(E) = 1 / [E \Sigma_t(E)], \quad (2)$$

where $\Sigma_t(E)$ the macroscopic total cross section. The group constants of the ABBN set were calculated under this assumption. The ETOX code also calculates the group constants following the assumption. Moreover, the isolated narrow-resonance approximation is used for unresolved resonance region. With this approach, the mutual interference effect between resonances of different nuclides and self-overlapping effect are ignored. Furthermore, the self-shielding of elastic removal cross section is assumed to be neglected.

On the other hand, the TIMS code calculates the effective cross section by solving numerically the neutron slowing down equation using the recurrence formula for slowing down source. The neutron slowing down equation in an infinite homogeneous system can be expressed as

$$\Sigma_t(u)\phi(u) = \sum_k S_k(u) = \sum_k \frac{1}{1-\alpha_k} \int_{u-\epsilon_k}^u e^{u'-u} \Sigma_{sk}(u')\phi(u')du' \quad , \quad (3)$$

$$\alpha_k = (A_k - 1)^2 / (A_k + 1)^2 \quad , \quad (4)$$

$$\epsilon_k = -\ln \alpha_k \quad , \quad (5)$$

where the subscript k stands for the nuclear species and $\phi(u)$ the neutron spectrum at lethargy u . On an ultrafine group representation, the slowing down source is easily shown to be written as⁽⁴⁾

$$S_k^m = S_k^{m-1} + \frac{\Delta u_m}{1+\alpha_k} (F_k^m - F_k^{m-L_k^m}) \quad , \quad (6)$$

$$F_k^m = \int_{\Delta u_m} \Sigma_{sk}(u)\phi(u)du = \Sigma_{sk}^m \phi^m \quad , \quad (7)$$

$$F_k^{m-L_k^m} = \int_{u-\epsilon_k}^{u_0-\epsilon_k} \Sigma_{sk}(u')\phi(u')du' \quad , \quad (8)$$

where u_0 is the lower bound of the $(m-1)$ -th fine group and L_k^m an integral number of groups which corresponds to the maximum lethargy gain by elastic collision.

The neutron spectrum on an ultrafine group m can be calculated numerically from Eqs.(3) and (6), when the Doppler broadened microscopic cross sections are provided on ultrafine group structure. Then, the effective group cross sections for capture, fission and elastic scattering are given by

$$\tilde{\sigma}_x = \frac{\sum \sigma_x^m \phi^m}{\sum \phi^m} \quad , \quad (9)$$

and the total and elastic removal cross sections are defined, respectively by

$$\tilde{\sigma}_t = \frac{\frac{\sum \phi^m}{\Delta E}}{\frac{\sum \frac{\phi^m}{\Delta E \sigma_{t,1}^m + R_0 \sigma_{t,2}^m + \sigma_0}}{\Delta E}} - \frac{\frac{\sum \phi^m}{\Delta E}}{\frac{\sum \frac{\phi^m}{\Delta E R_0 \sigma_{t,2}^m + \sigma_0}}{\Delta E}} \quad (10)$$

and

$$\tilde{\sigma}_{er} = \frac{\frac{\sum \sigma_n^m \phi^m \frac{E_L - \alpha E_m}{(1-\alpha)E_m}}{\Delta E'}}{\frac{\sum \phi^m}{\Delta E}}, \quad (11)$$

where $\Delta E' = E_L/\alpha - E_L$, $\sigma_{t,1}$ the total cross section of the resonant nuclei under consideration, $\sigma_{t,2}$ that of the other resonant material, R_0 the atomic density ratio of the nuclei (2) to (1), E_L the lower group energy boundary of integration interval ΔE and σ_0 the admixture background scattering cross section of Bondarenko's type.

The numerical calculations were performed by assuming the average moderator mass $A_k = 30$.⁽³⁾ The resulting group constants for ^{235}U , ^{238}U , ^{239}Pu , ^{240}Pu and ^{241}Pu are shown as tables of the JAERI Fast set format in Appendix.

The self-shielding factors calculated with the TIMS and ETOX codes are compared for some typical energy groups in Figs.1.0 ~ 5.8.

Figures 1.0 ~ 1.10 show the comparison of the self-shielding factors for fission cross sections of ^{235}U . The differences between the self-shielding factors obtained by TIMS and ETOX are considerably observed from these figures. The composition dependence of the self-shielding factors calculated by the TIMS code is larger than that obtained by the ETOX code, as seen from Fig.1.0. The temperature coefficients of the self-shielding factors are also different between the results of TIMS and ETOX. For the

ETOX results, especially, the temperature dependence is negligibly small in the high energy groups. Furthermore it should be noticed that the magnitude of the temperature coefficient of self-shielding factors changes between the TIMS and ETOX results according to the change in σ_0 -values. As seen from Fig.1.6, for example, the temperature dependence of self-shielding factors calculated by ETOX is larger than the one obtained by TIMS for $\sigma_0 = 10$ (barns), but the temperature dependence becomes inversely small for $\sigma_0 = 1000$ (barns) in the high energy groups.

In Figs.2.0 ~ 2.7, the self-shielding factors for capture cross sections of ^{238}U are compared for several energy groups. The temperature dependence of self-shielding factors calculated by ETOX is larger than the one by TIMS for the case of $\sigma_0 = 10$ barns in the unresolved energy groups. This tendency can be seen also for the case of $\sigma_0 = 1000$ barns.

This fact differs from the result described above for ^{235}U , which may be attributed to the difference in the expression of resonance cross section. In the TIMS code, Doppler broadened cross sections of ^{238}U and ^{240}Pu were calculated by a multilevel formula⁽¹²⁾ to avoid unreasonable result produced by adding the floor correction cross sections to the Breit-Wigner single-level expression, as shown in Fig.6.

In Figs.3.0 ~ 3.9, the self-shielding factors for fission cross sections of ^{239}Pu are compared for several energy groups. The comparison results can be similarly summarized to those observed for ^{235}U mentioned above.

In Figs.4.0 ~ 4.5 and Figs.5.0 ~ 5.8, the self-shielding factors of ^{240}Pu and ^{241}Pu are compared for several energy groups, respectively. It is observed also for this case that the difference between the self-shielding factors calculated with the two different methods are remarkable and each method gives a different temperature dependence of self-shielding

factors.

In the next chapter, thus, we study the effects of these differences between the self-shielding factors calculated with TIMS and ETOX codes on the integral quantities in fast reactor system.

In Figs.7 ~ 18, the Doppler broadened cross sections of ^{238}U and ^{239}Pu calculated with the TIMS code are shown for several energy ranges. The change of resonance cross sections broadened by temperature raising from 300 °K to 900 or 2100 °K can be intuitively known for the resolved and unresolved ranges from these figures.

3. Comparison of Integral Quantities Calculated by Two Group Cross Section Sets Obtained from TIMS and ETOX Methods

The differences between two group constants sets obtained from the TIMS and ETOX codes exist only in the effective group cross sections of heavy nuclides in the resonance energy regions. As integral quantities to be studied, we selected the effective multiplication factor (k_{eff}), Doppler reactivity effect and sodium void reactivity effect. Main characteristics of fast reactor critical assemblies used for this comparison calculation of these integral quantities are summarized in Table 1. Assembly FCA-VI-1 is the physics mockup core of JOYO (Experimental Fast Reactor). The SEFOR assembly is the testing core for both static power reactivity and rapid super-prompt-critical reactivity measurements. In the present analysis, the experimental isothermal Doppler coefficient was calculated with the use of the benchmark specification model.⁽¹³⁾ The assemblies, ZPPR-2 and ZPR-6-7 are the demonstration fast reactor benchmark cores to provide physics data necessary for LMFBR design.

The neutronics calculations of the integral quantities were performed with the use of diffusion theory code, DOPP2D⁽¹⁴⁾ using two group constants sets of JENDL-TIMS and JENDL-ETOX with the 70 group structure.

3.1 Effective Multiplication Factor

The effective multiplication factors were calculated with the two-dimensional R-Z homogeneous model. The difference between JENDL-ETOX and JENDL-TIMS is very small and below about 0.2 %, as shown in Table 2. Hence, the difference between the two calculational methods for the group constants may be negligibly small for the k_{eff} calculation.

3.2 Sodium Void Reactivity Effect

The experimental results of sodium void reactivity effect in ZPPR assembly 2 have been analysed with one-dimensional spherical homogeneous model. The sodium-voided zone consists of 93 matrix positions with all voided 12 inches each half core. In the present analysis, some important corrections such as two-dimensional, heterogeneity and neutron streaming effects were not considered, because the present aim lines only in studying the influence of two different calculational methods for group constants on sodium void effect.

Table 3 shows the comparison of the sodium void reactivity separated to each component term. The difference between JENDL-TIMS and JENDL-ETOX is negligible small for the total reactivity, though the difference by about 11 % is observed for " $\nu\Sigma_f$ " component term.

3.3 Doppler Reactivity Effect

The temperature dependence of the group cross sections calculated by the two different codes, TIMS and ETOX, has been tested from the analyses of Doppler experiments performed in ZPPR-2 and SEFOR assemblies. The experiment in ZPPR-2 was the sample Doppler reactivity measurement for the natural UO_2 (NUO_2), and in SEFOR assembly was the measurement of the isothermal Doppler coefficient for the full core.

The results analysed for the NUO_2 sample Doppler experiment in ZPPR assembly 2 are shown in Fig.19. The calculation was performed with the one-dimensional first-order perturbation theory. The temperature dependence of group cross sections of ^{238}U can be tested from this experimental analysis. Both the results calculated with the use of JENDL-TIMS and -ETOX are larger than the experimental values by 10 ~ 14 %. The results of JENDL-TIMS and -ETOX are in a very good agreement with each other, but

the values of ETOX are larger than those of TIMS by 1 ~ 2 %, although the comparison of the groupwise Doppler reactivity effect indicates remarkable discrepancies between the results of JENDL-TIMS and JENDL-ETOX. It is observed that JENDL-ETOX results are larger than JENDL-TIMS ones in the unresolved resonance region and reversely small in the resolved region. This tendency observed produces an accidental cancellation and gives a good agreement between the results of JENDL-TIMS and -ETOX for the total Doppler reactivity.

The results analysed for the Doppler reactivity measurement of the full core in SEFOR assembly are compared in Figs.20 and 21. This analysis was performed with the first-order perturbation theory using two-dimensional R-Z benchmark model. The results of JENDL-TIMS and -ETOX overestimate the experimental values by 19 % and 23 %, respectively. In both the results, the positive Doppler reactivity by fission component term is more than 30 % in comparison with the negative one by capture term. The difference in the fission component between JENDL-TIMS and -ETOX is remarkable as seen from Fig.21, and the result of JENDL-TIMS is larger than the one of JENDL-ETOX, especially in the unresolved region. This tendency differs from the results for the capture component as shown in Fig.20. The tendency for the capture term is similar to the results of the NUO_2 sample Doppler analysis indicated in Fig.19, because the total capture component contributes dominantly to the ^{238}U Doppler effect. These different tendencies for $\nu\Sigma_f$ - and Σ_c -terms between JENDL-TIMS and -ETOX can be comprehended by observing Figs.1.1 ~ 5.8. These figures show that the magnitude of the temperature dependence of the group cross sections calculated with two different methods differs between TIMS and ETOX results, depending on the σ_0 -values, as described in Chapter 2. For example, as seen from Fig.1.6, the temperature dependence of self-shielding factors calculated

by ETOX is larger than the one by TIMS for $\sigma_0 = 10$ (barns), but the magnitude of the temperature dependence becomes inversely small for $\sigma_0 = 1000$ (barns) in the unresolved resonance region. The values of σ_0 for ^{238}U are commonly less than 100 barns and those for ^{239}Pu more than 100 barns for typical core compositions. However, the comparison of the total Doppler reactivities shows that the difference between the results of JENDL-TIMS and -ETOX is very small because of the eventual cancellation mentioned above.

4. Concluding Remarks

Some integral quantities, k_{eff} , Na-void reactivity and Doppler reactivity effects, were calculated by using the two different group cross sections sets, which were produced with the different methods of TIMS and ETOX codes. The calculated values were compared with each other and the results are summarized as follows: The values obtained from these two sets are in a good agreement with each other. However, as for the Doppler effect of the effective cross sections, the difference between the results of TIMS and ETOX depends strongly on the energy groups and the compositions. A good agreement between the results of the Doppler reactivity effects from JENDL-TIMS and -ETOX methods is considered to be due to the eventual cancellation. Hence, it cannot be concluded that the difference between the TIMS and ETOX methods to the Doppler effect is always negligibly small for any fast reactor systems. This remark will become more clear if the mutual interference effect⁽¹⁴⁾⁽¹⁵⁾ is taken into account for the calculation of the self-shielding factors in the TIMS method. Moreover, the present remark will be an interesting problem for neutronics calculations of heterogeneous² composed core reactors, because each core region may produce different Doppler coefficient.

Acknowledgments

The authors would like to express their gratitude to Mr. A. Hasegawa of JAERI and Mr. Y. Nishio of JAIS for their valuable suggestions and helps in the present work, and they wish to thank to members of Japan Nuclear Data Center in JAERI for their sincere guides about the JENDL-1 nuclear data file.

The production of 70-group constants for the JENDL-1 data was performed under the auspices of Power Reactor and Nuclear Fuel Development Corporation.

References

- (1) ABAGJAN L.P., et al.: "Group Constants for Nuclear Reactor Calculation", Consultants Bureau, New York (1964).
- (2) KATSURAGI S., TONE T., HASEGAWA A.,: JAERI 1195 (1970).
- (3) KATSURAGI S., ISHIGURO Y., TAKANO H., et al.: JAERI 1199 (1970).
- (4) TAKANO H., HASEGAWA A., NAKAGAWA M., et al.: JAERI 1255 (1978).
- (5) WRIGHT R.Q., GREENE N.M., et al.: ORNL-TM-2679.
- (6) TONE T., et al.: JAERI 1192 (1970).
- (7) HASEGAWA A., et al.: to be published.
- (8) SCHETER R.E., BAKER J.L., KIDMAN R.B.: BNWL-1002 (1969).
- (9) TAKANO H., et al.: to be published.
- (10) IGARASHI S., et al.: to be published.
- (11) TAKANO H., et al.: J. Nucl. Sci. Technol., 7[10], 500 (1970).
- (12) TAKANO H., ISHIGURO Y.: J. Nucl. Sci. Technol., 14[9], 627 (1977).
- (13) HARISS R.A.: HEDL-TME 73-42 (1973).
- (14) TAKANO H., MATSUI Y.: "Analysis of Doppler Effect with JAERI-Fast Set", JAERI-M 7195 (1977).
- (15) TAKANO H., ISHIGURO Y., MATSUI Y.: 1977 Fall Meeting of the Atomic Energy Society of Japan, F16, P304 (1977)(in Japanese).

Table 1. Main characteristics of fast reactor critical assemblies

Assembly	Fuel	R = Fertile/Fissile		Core volume(ℓ)
		Inner core	Outer core	
FCA-VI-1	Pu, U	4.3	3.0	223
SEFOR	Pu	4.3		558
ZPPR-2	Pu	6.5	4.0	2400
ZPR-6-7	Pu	6.5	6.5	3120
LMFBR*	Pu	8.7	6.6	5000

* Large sodium-cooled fast breeder reactor for an international comparison calculation.

Table 2 Effective multiplication factors calculated by the DOPP2D code for 2-dimensional R-Z model

Set Assembly	JENDL-TIMS	JENDL-ETOX	TIMS/ETOX
FCA-VI-1	0.99797	0.99819	0.9998
ZPPR-2 L-90(normal)	0.99135	0.99275	0.9986
ZPR-6-7 (H240)	0.99022	0.99134	0.9989
LMFBR (Na-in)	1.02372	1.02494	0.9988
SEFOR	1.02327	1.02332	0.9999

Table 3. Central Na-void reactivity by 70-group
1-dimensional 1-st order perturbation
calculation in ZPPR-2 Assembly

Component \ Set	JENDL-TIMS	JENDL-ETOX	Difference between TIMS and ETOX
ΔK by $\nu\Sigma_f$	-3.632 -5	-3.281 -5	-3.51 -6
ΔK by Σ_r	3.556 -3	3.340 -3	2.16 -4
ΔK by Σ_a	1.134 -3	1.112 -3	2.20 -5
ΔK by Σ_{in}	3.340 -3	3.326 -3	1.40 -5
ΔK by D	-4.884 -4	-4.826 -4	-5.80 -6
Total reactivity	7.505 -3	7.262 -3	2.43 -4

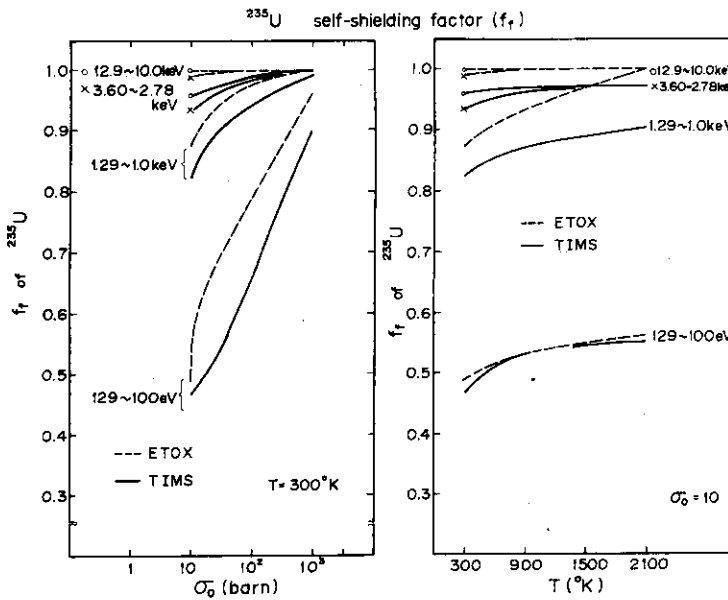


Fig. 1.0 Comparison of fission self-shielding factors of ^{235}U calculated with the TIMS and ETOX codes

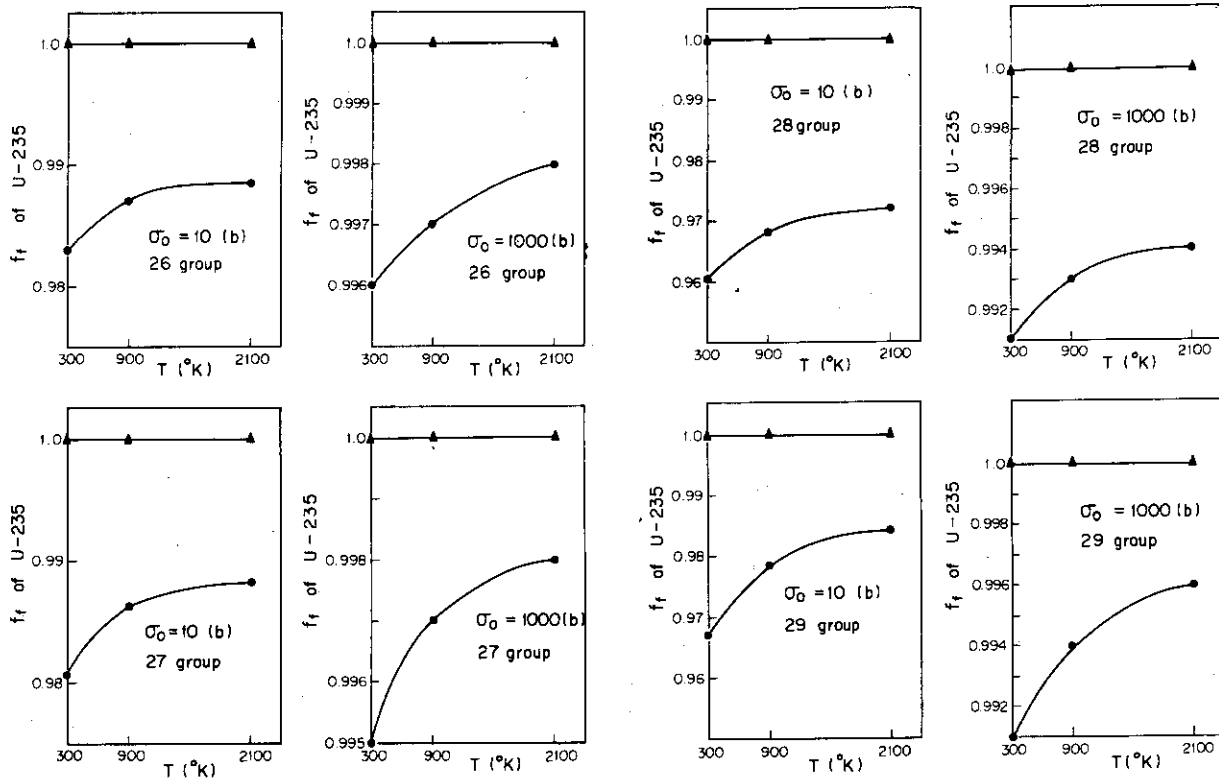


Fig. 1.1 Comparison of fission self-shielding factors of ^{235}U .
 ● : TIMS, ▲ : ETOX

Fig. 1.2 Comparison of self-shielding factors of ^{235}U .
 ● : TIMS, ▲ : ETOX

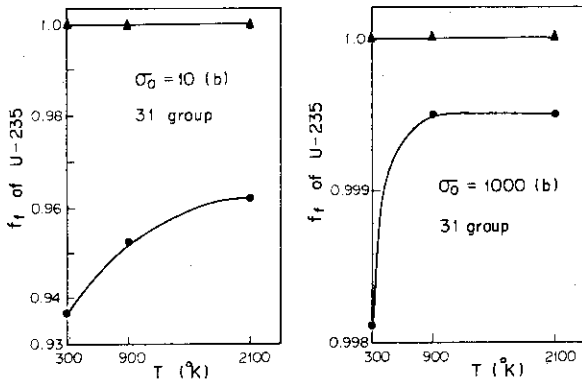
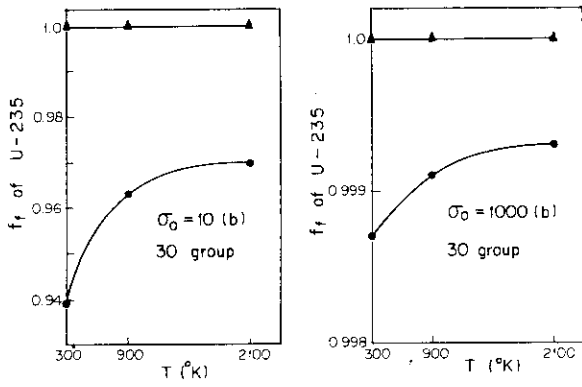


Fig. 1.3. Comparison of self-shielding factors of ^{235}U ,
 ● : TIMS, ▲ : ETOX

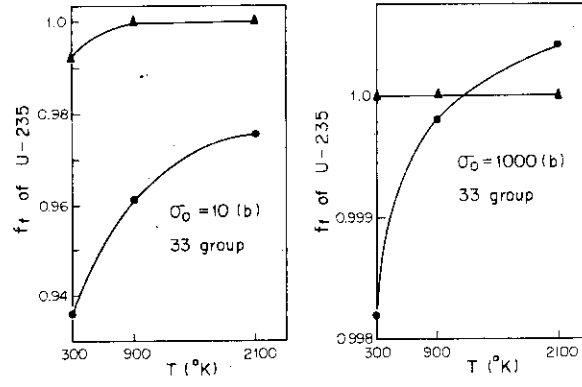
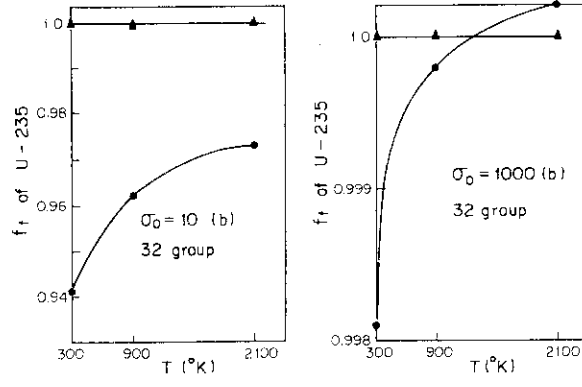


Fig. 1.4. Comparison of self-shielding factors of ^{235}U ,
 ● : TIMS, ▲ : ETOX

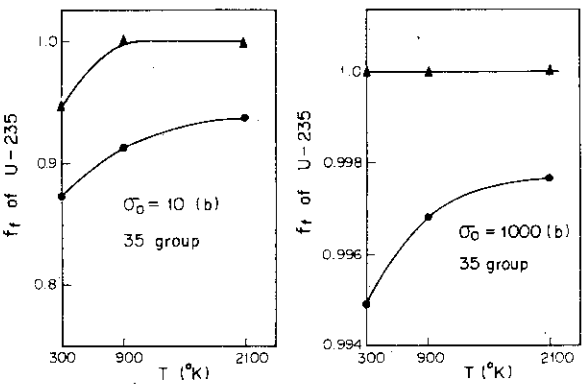
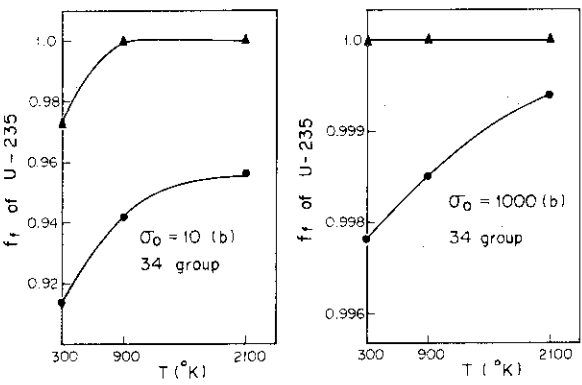


Fig. 1.5. Comparison of self-shielding factors of ^{235}U ,
 ● : TIMS, ▲ : ETOX

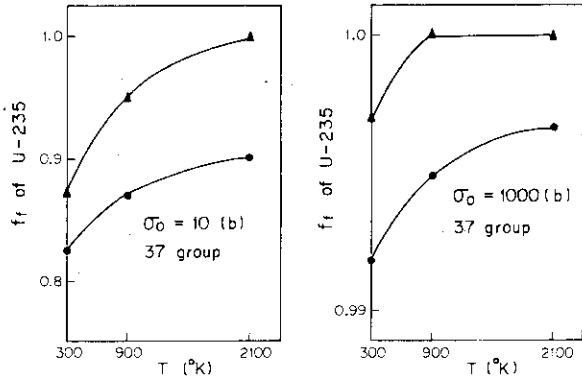
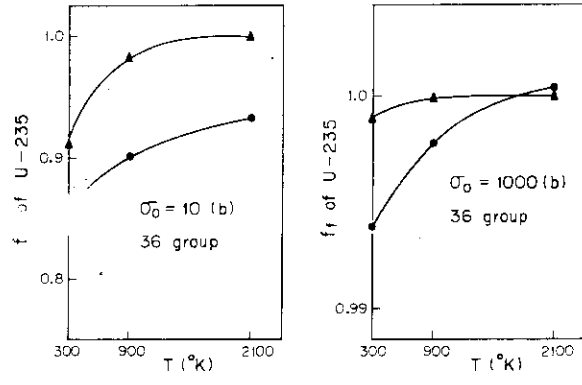


Fig. 1.6. Comparison of self-shielding factors of ^{235}U ,
 ● : TIMS, ▲ : ETOX

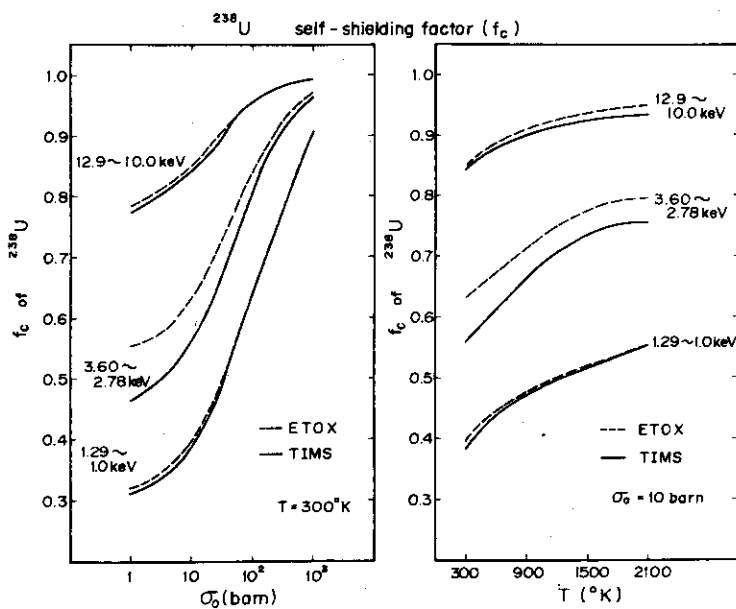


Fig. 2.0 Comparison of capture self-shielding factors of ^{238}U calculated with the TIMS and ETOX codes

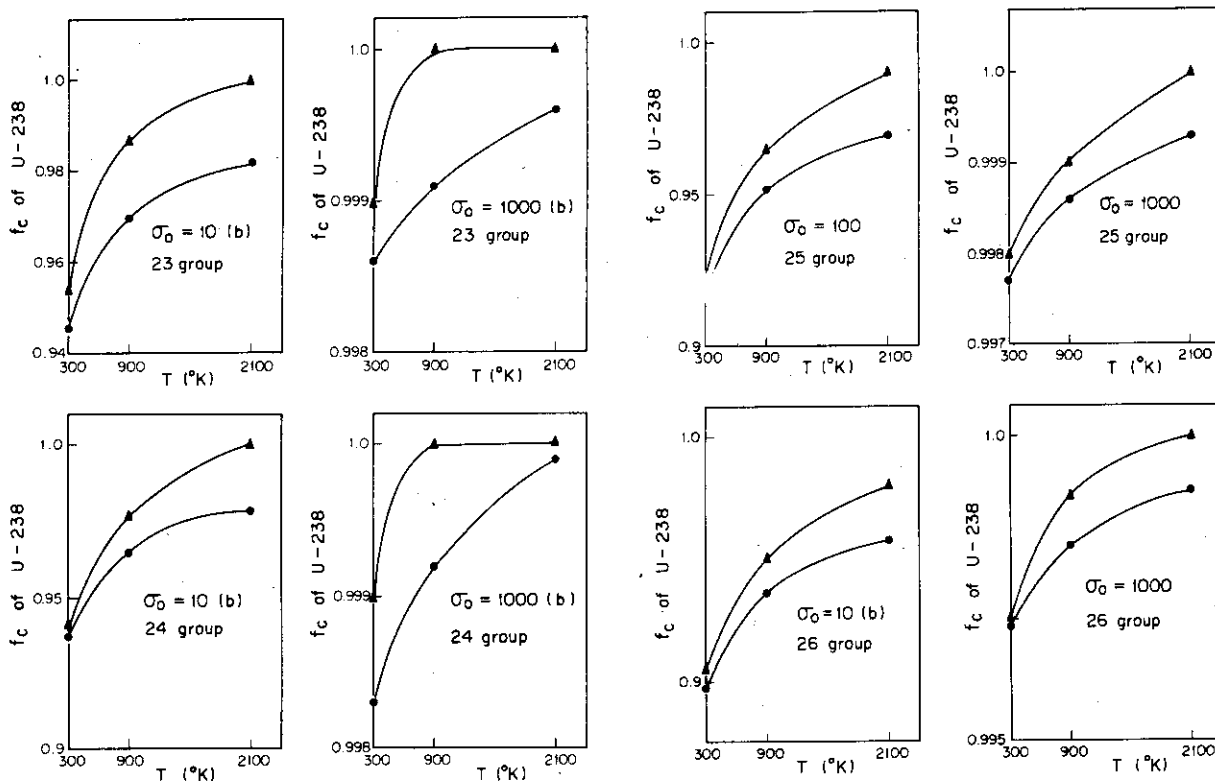


Fig. 2.1 Comparison of capture self-shielding factors of ^{238}U ,
 ● : TIMS, ▲ : ETOX

Fig. 2.2 Comparison of capture self-shielding factors of ^{238}U ,
 ● : TIMS, ▲ : ETOX

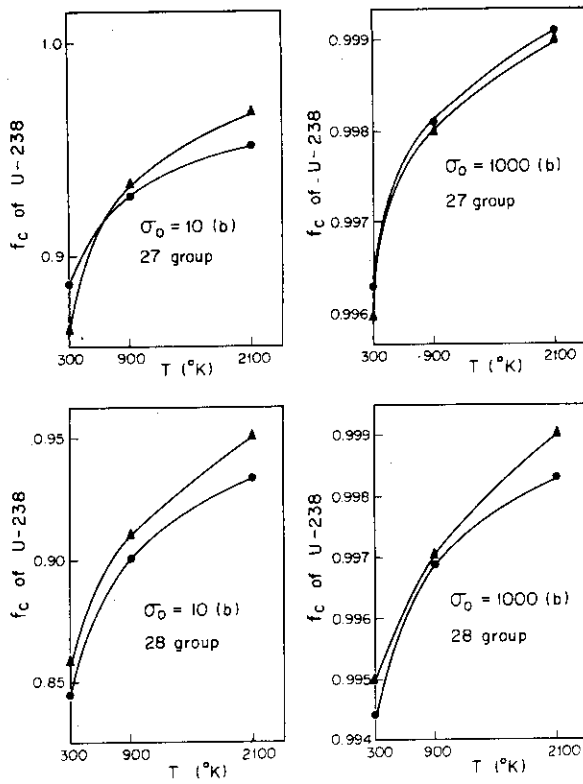


Fig. 2.3 Comparison of capture self-shielding factors of ²³⁸U.
 ● : TIMS, ▲ : ETOX

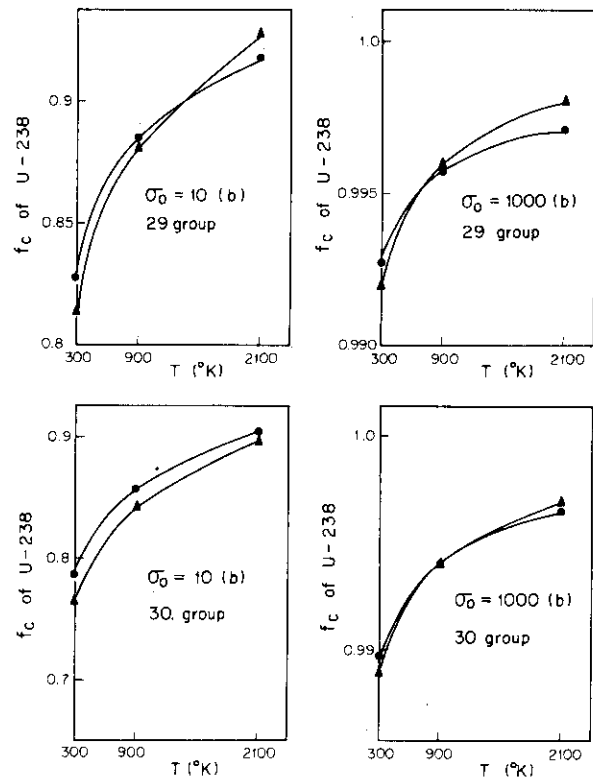


Fig. 2.4 Comparison of capture self-shielding factors of ²³⁸U.
 ● : TIMS, ▲ : ETOX

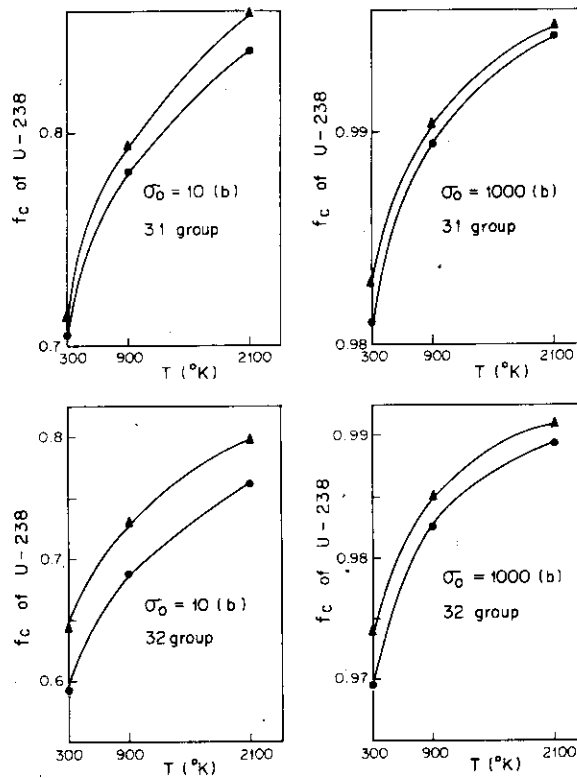


Fig. 2.5 Comparison of capture self-shielding factors of ²³⁸U.
 ● : TIMS, ▲ : ETOX

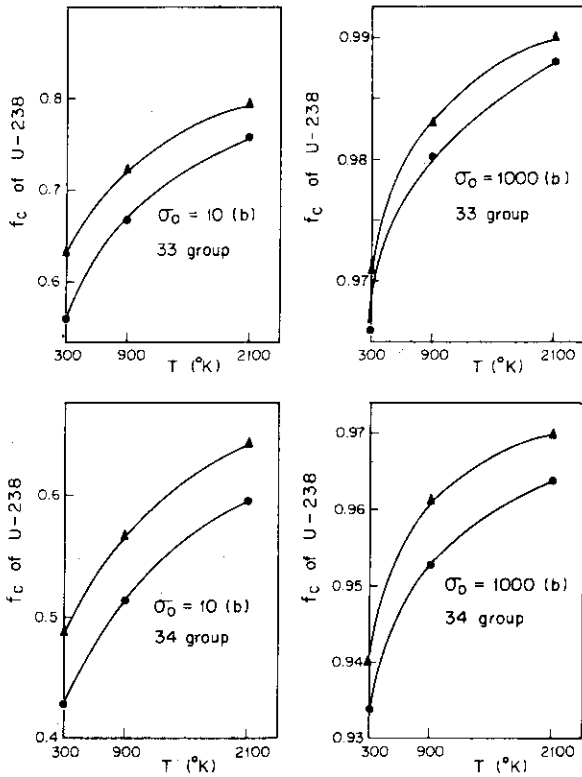


Fig. 2.6. Comparison of capture self-shielding factors of ^{238}U ,
 ● : TIMS, ▲ : ETOX

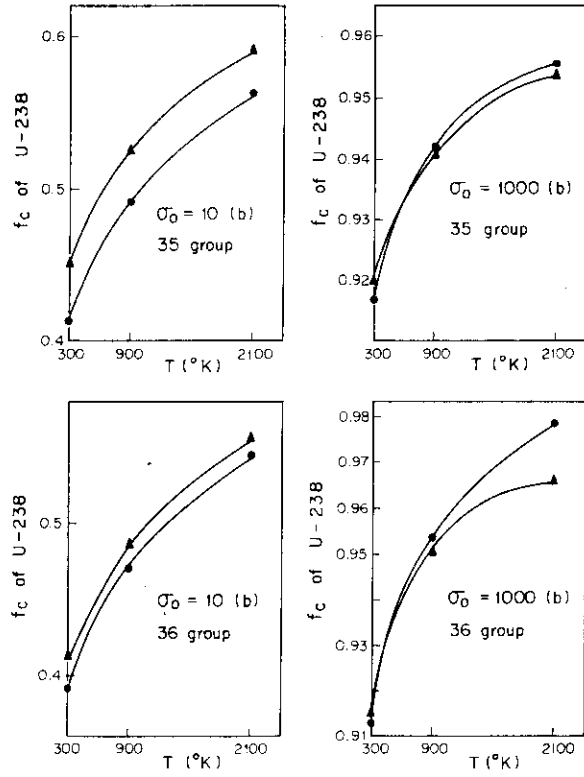


Fig. 2.7. Comparison of capture self-shielding factors of ^{238}U ,
 ● : TIMS, ▲ : ETOX

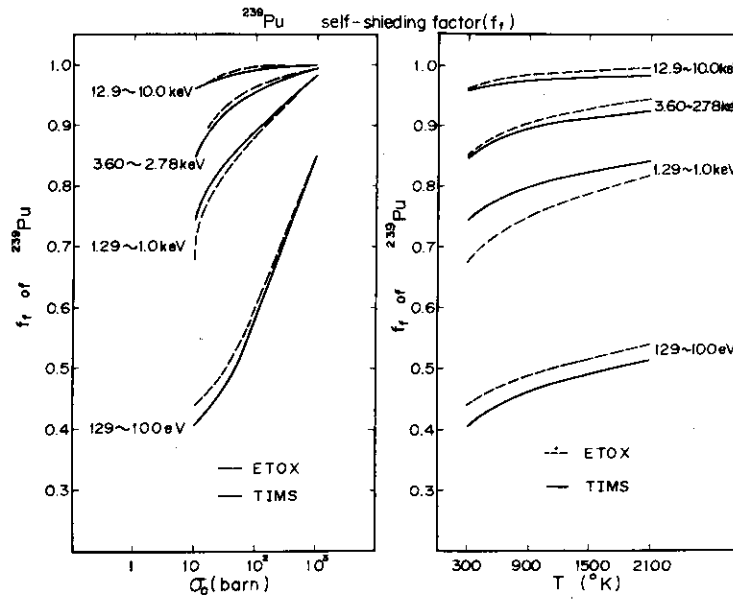


Fig. 3.0 Comparison of fission self-shielding factors of ^{239}Pu calculated with the TIMS and ETOX codes

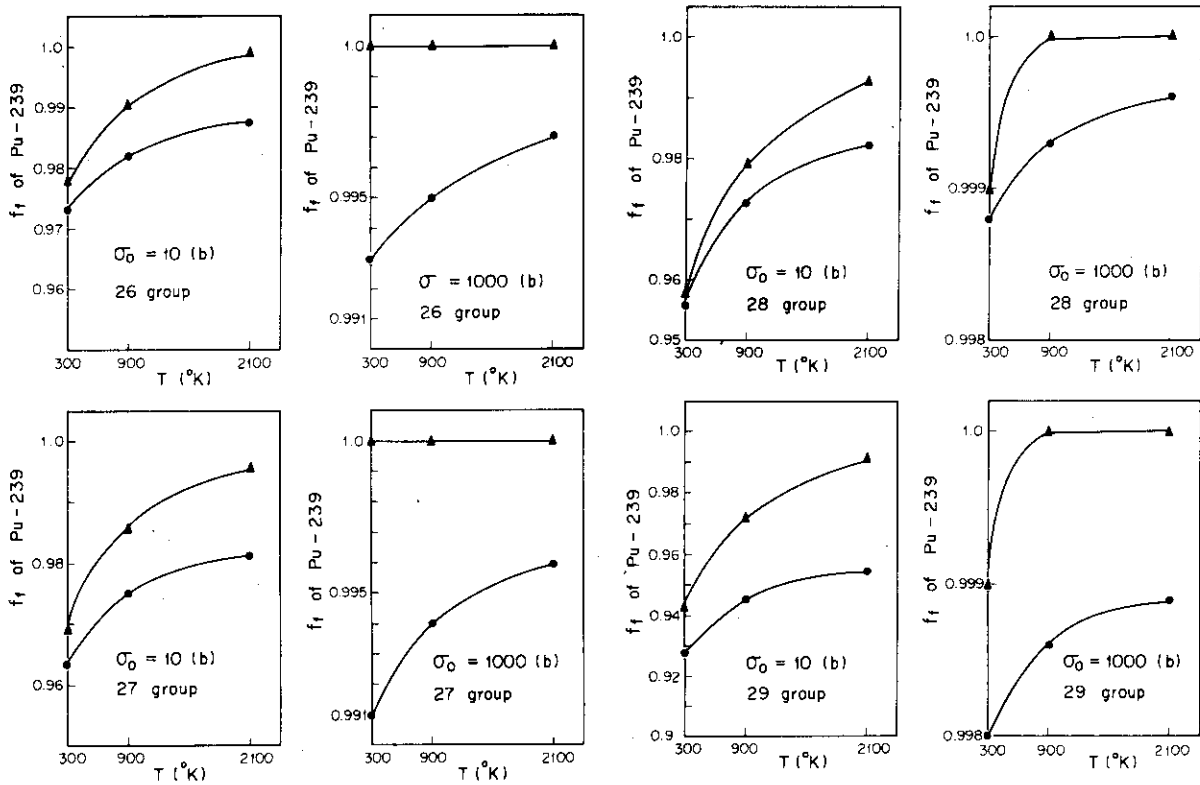


Fig. 3.1 Comparison of fission self-shielding factors of ^{239}Pu ,
 ● : TIMS, ▲ : ETOX

Fig. 3.2 Comparison of fission self-shielding factors of ^{239}Pu ,
 ● : TIMS, ▲ : ETOX

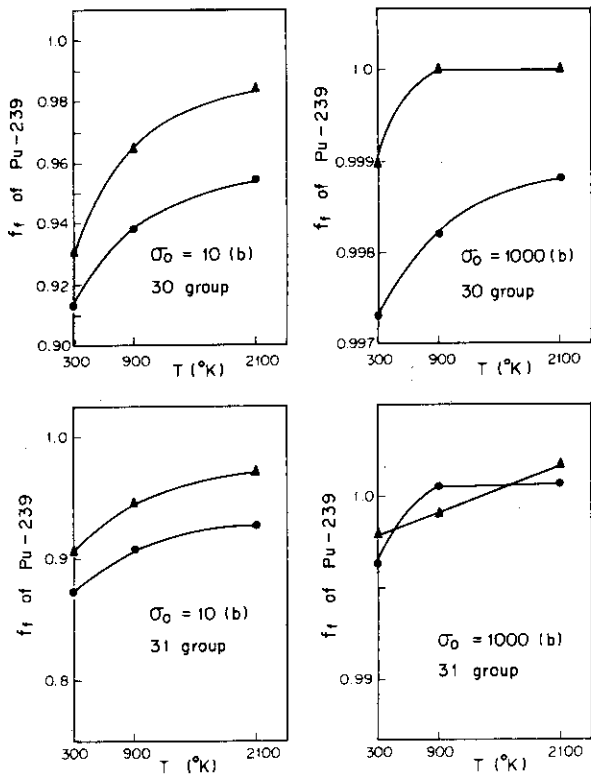


Fig. 3.3. Comparison of fission self-shielding factors of ^{239}Pu .
 ● : TIMS, ▲ : ETOX

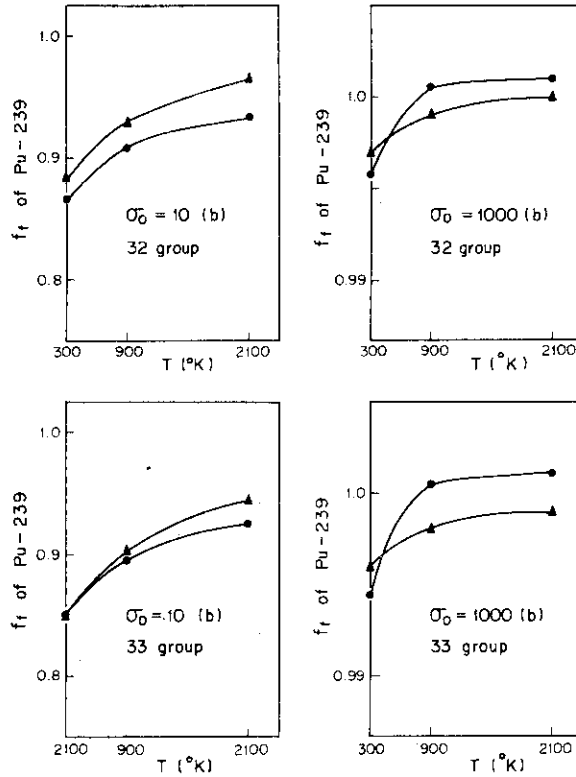


Fig. 3.4. Comparison of fission self-shielding factors of ^{239}Pu .
 ● : TIMS, ▲ : ETOX

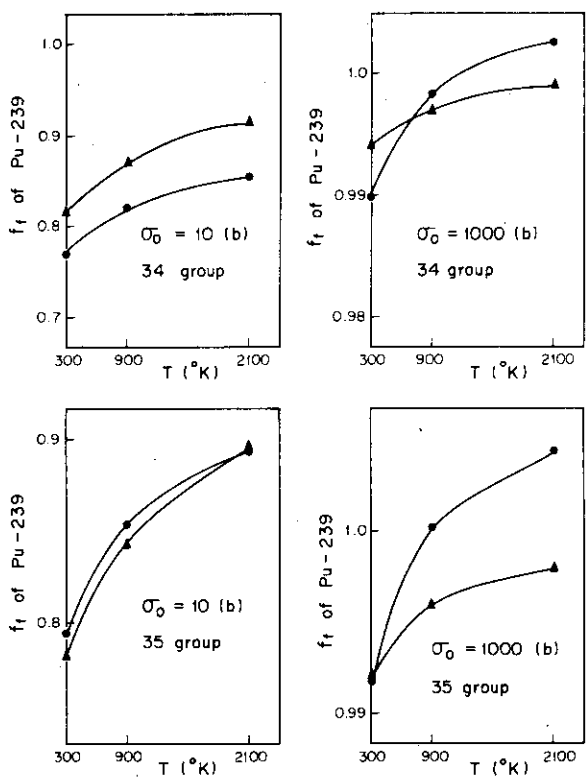


Fig. 3.5. Comparison of fission self-shielding factors of ^{239}Pu .
 ● : TIMS, ▲ : ETOX

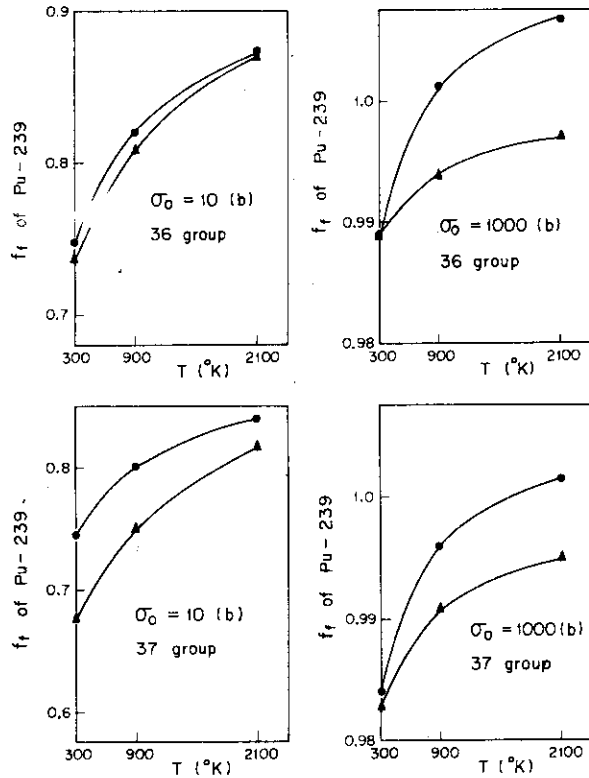


Fig. 3.6. Comparison of fission self-shielding factors of ^{239}Pu .
 ● : TIMS, ▲ : ETOX

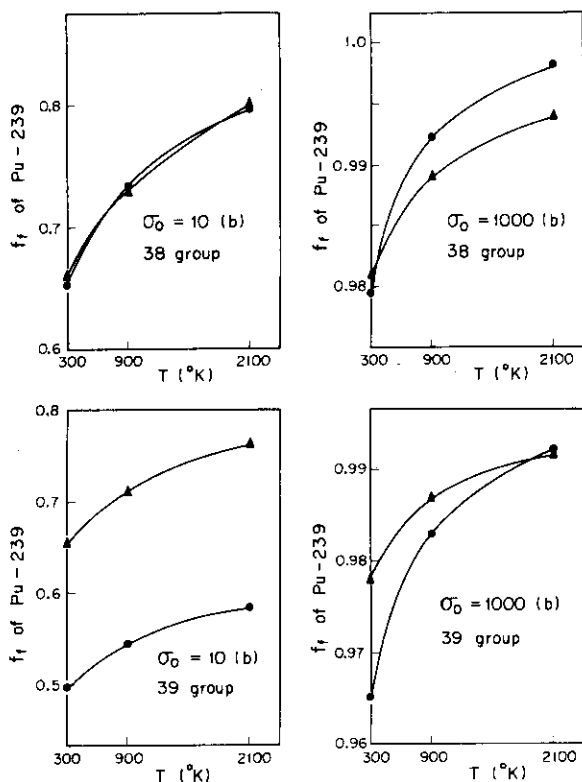


Fig. 3.7. Comparison of fission self-shielding factors of ^{239}Pu
 ● : TIMS, ▲ : ETOX

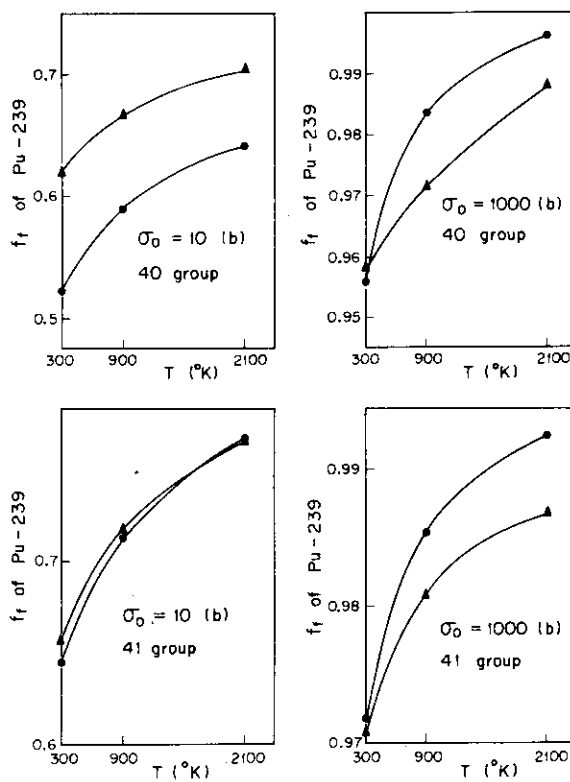


Fig. 3.8. Comparison of fission self-shielding factors of ^{239}Pu
 ● : TIMS, ▲ : ETOX

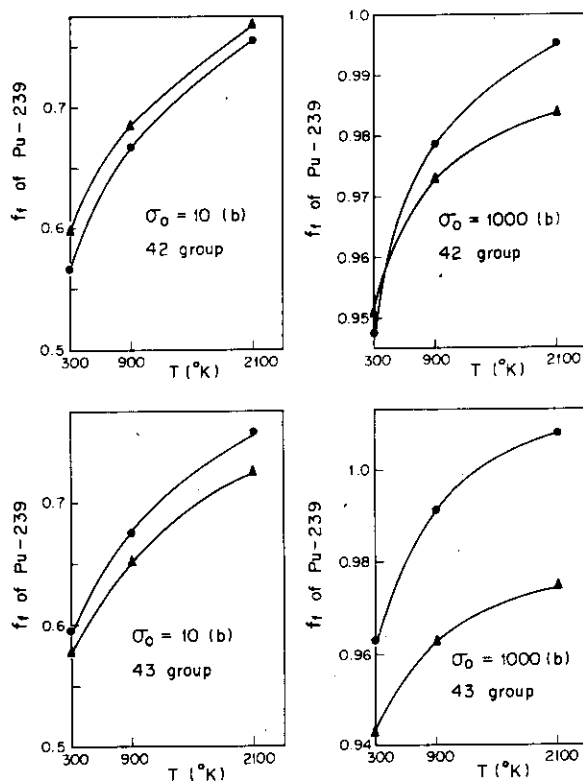


Fig. 3.9. Comparison of fission self-shielding factors of ^{239}Pu .
 ● : TIMS, ▲ : ETOX

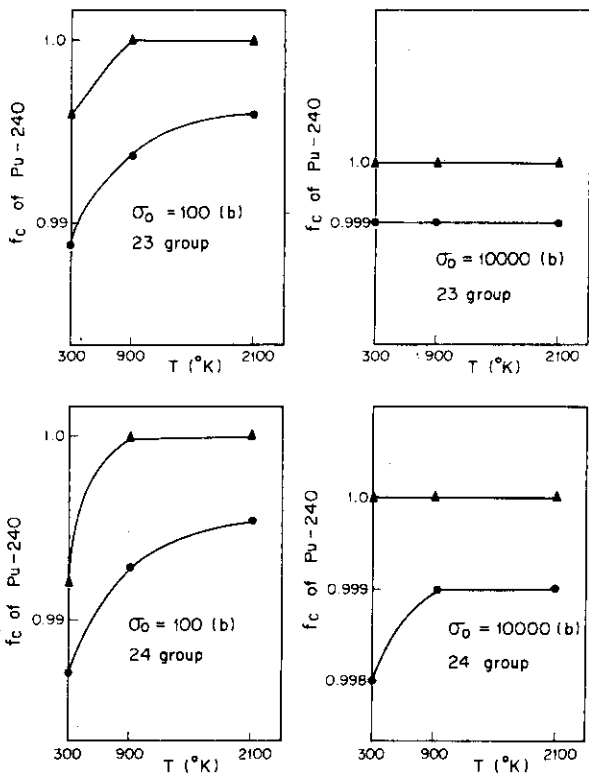


Fig. 4.1 Comparison of capture self-shielding factors of ^{240}Pu .
 ● : TIMS, ▲ : ETOX

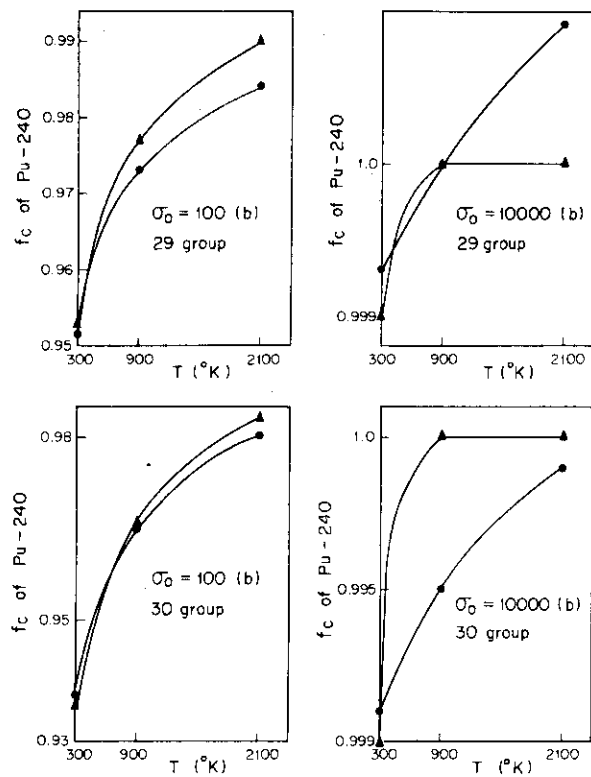


Fig. 4.2 Comparison of capture self-shielding factors of ^{240}Pu .
 ● : TIMS, ▲ : ETOX

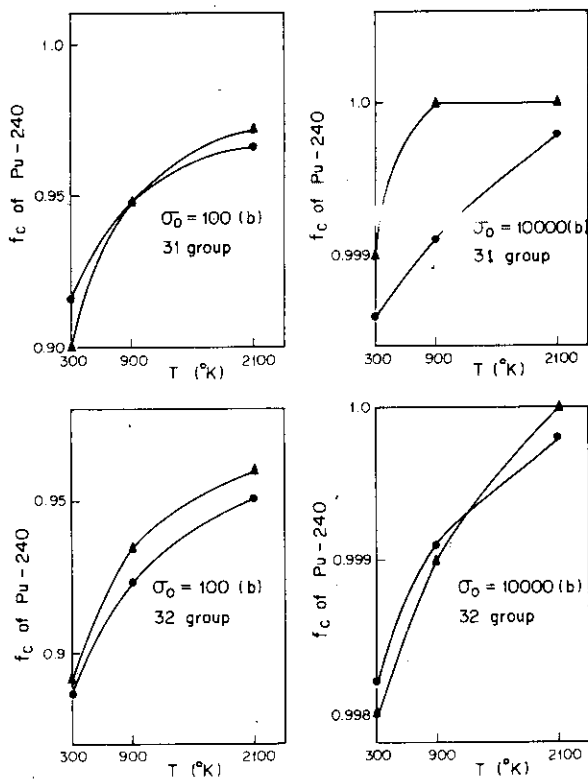


Fig. 4.3 Comparison of capture self-shielding factors of ^{240}Pu .
 ● : TIMS, ▲ : ETOX

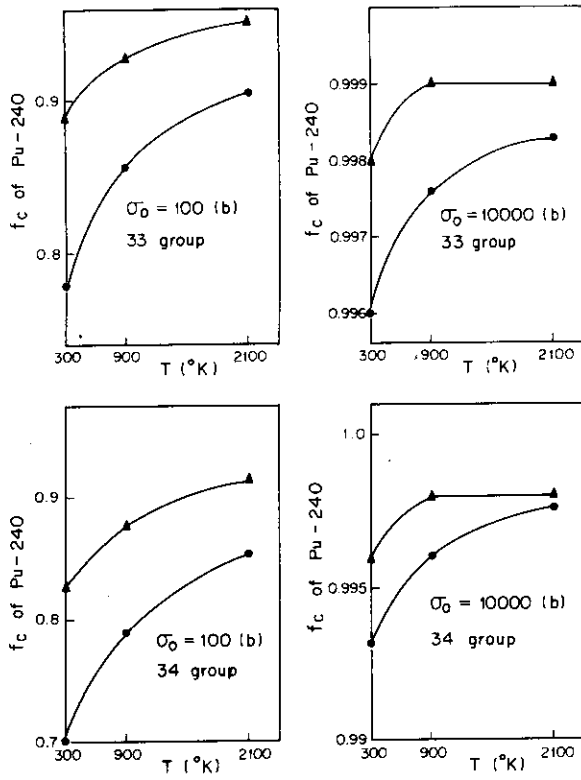


Fig. 4.4. Comparison of capture self-shielding factors of ^{240}Pu .
 ● : TIMS, ▲ : ETOX

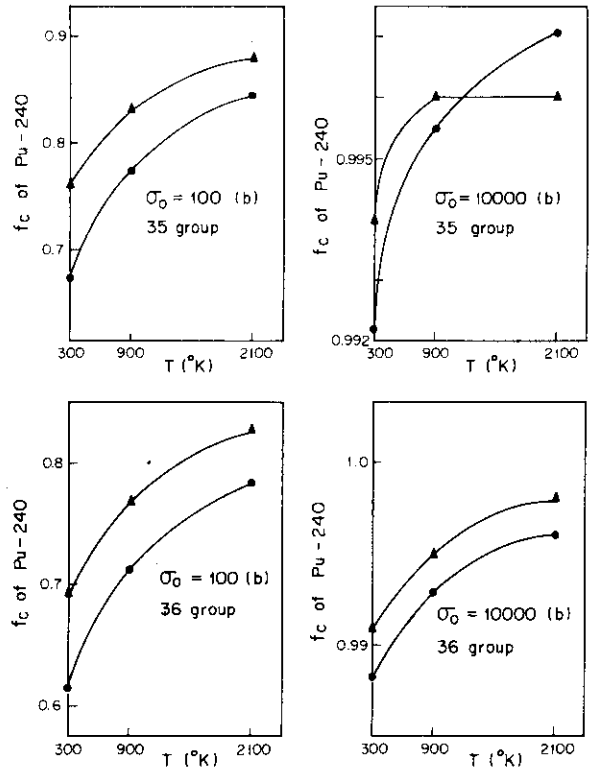


Fig. 4.5. Comparison of capture self-shielding factors of ^{240}Pu .
 ● : TIMS, ▲ : ETOX

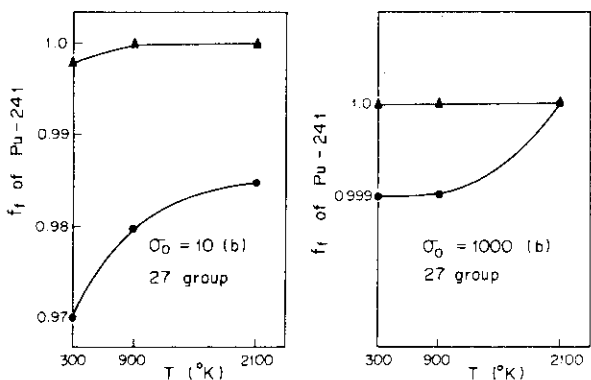
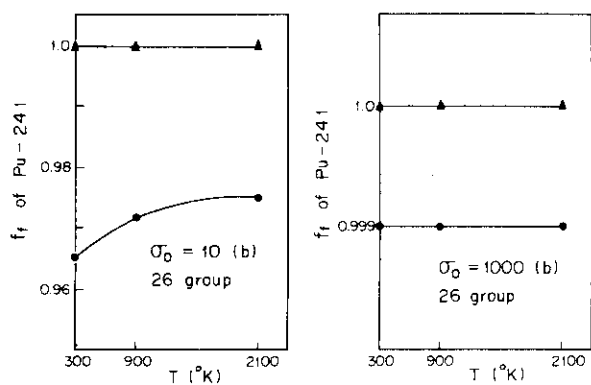


Fig. 5.1. Comparison of fission self-shielding factors of ^{241}Pu ,
 ● : TIMS, ▲ : ETOX

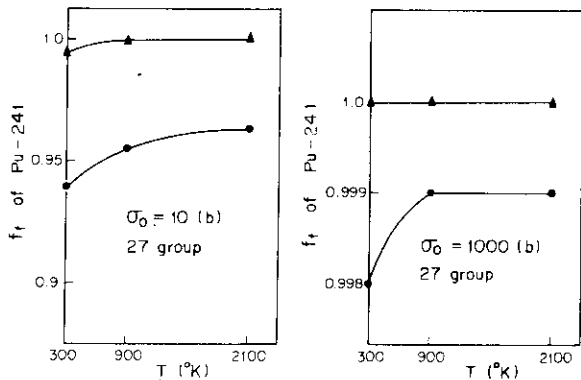
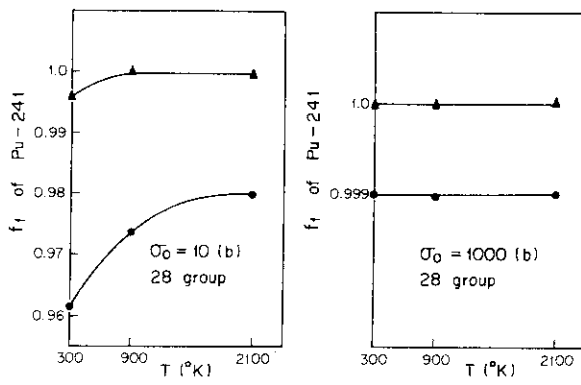


Fig. 5.2. Comparison of fission self-shielding factors of ^{241}Pu ,
 ● : TIMS, ▲ : ETOX

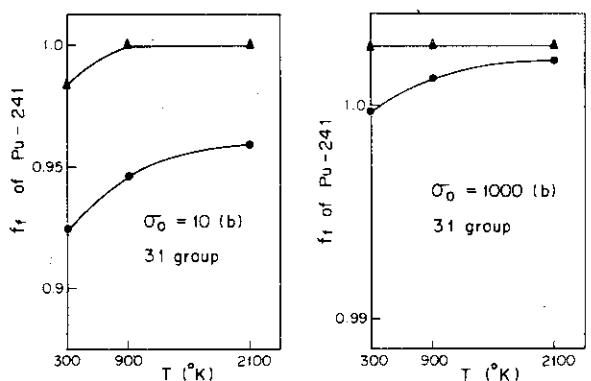
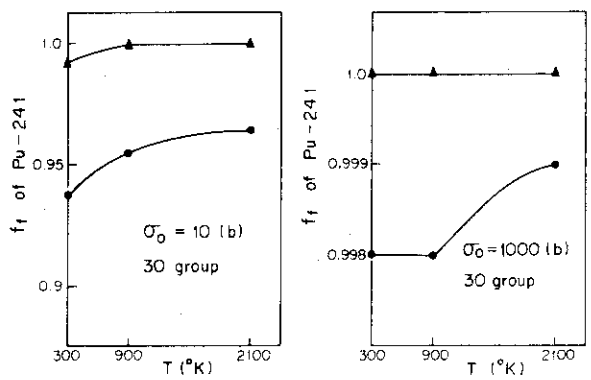


Fig. 5.3. Comparison of fission self-shielding factors of ^{241}Pu ,
 ● : TIMS, ▲ : ETOX

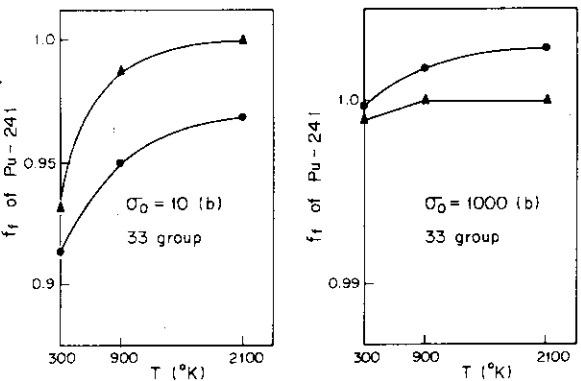
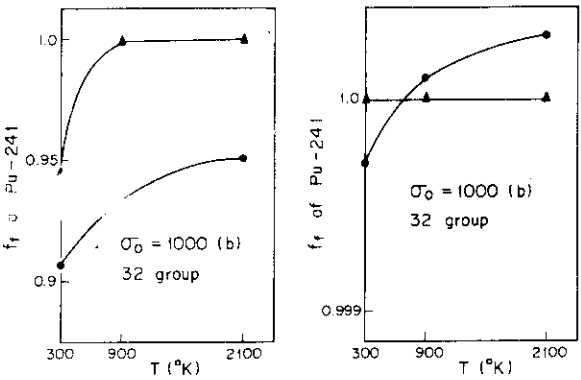


Fig. 5.4. Comparison of fission self-shielding factor of ^{241}Pu ,
 ● : TIMS, ▲ : ETOX

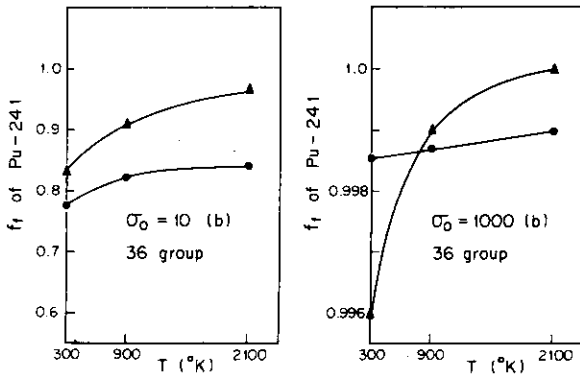


Fig. 5.5. Comparison of fission self-shielding factors of ²⁴¹Pu,
●—● : TIMS, ▲—▲ : ETOX

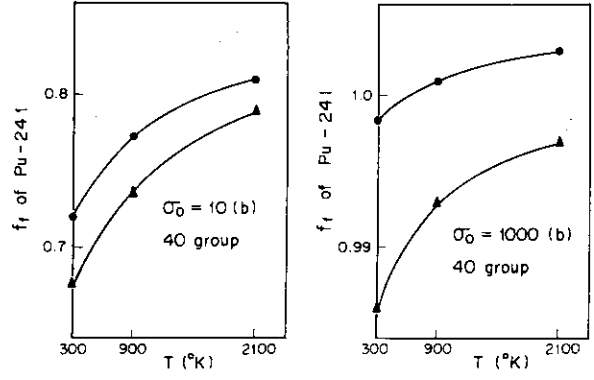


Fig. 5.6. Comparison of fission self-shielding factors of ²⁴¹Pu,
●—● : TIMS, ▲—▲ : ETOX

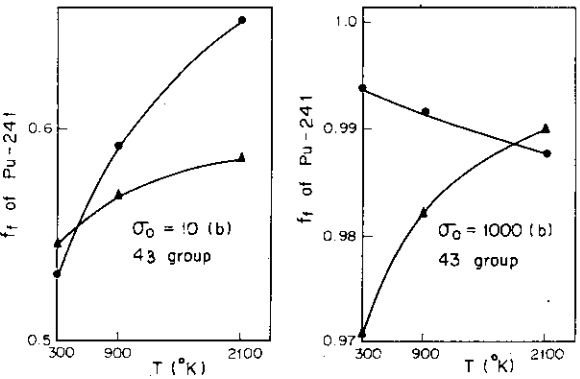
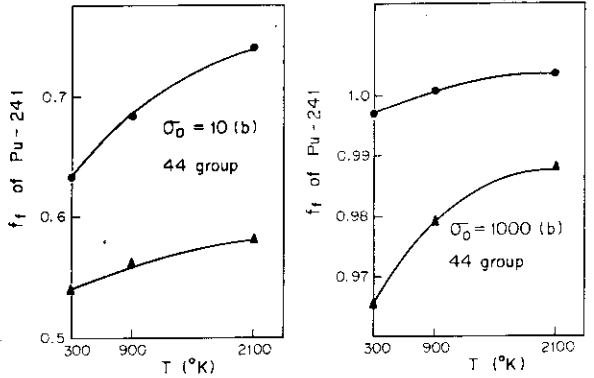
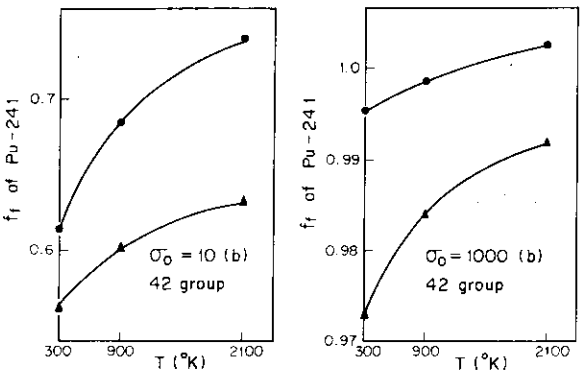
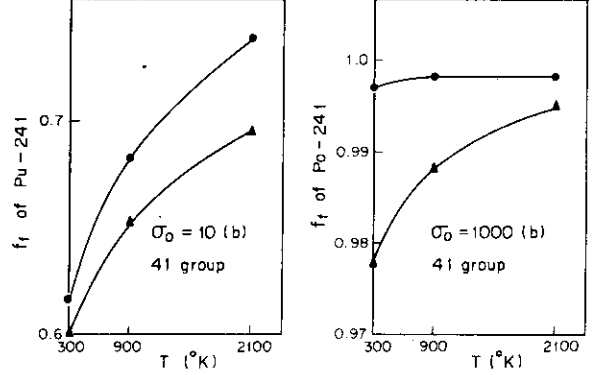
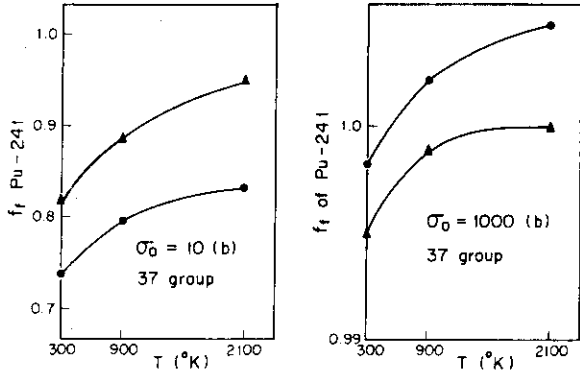


Fig. 5.8. Comparison of fission self-shielding factors of ²⁴¹Pu,
●—● : TIMS, ▲—▲ : ETOX

Fig. 5.7. Comparison of fission self-shielding factors of ²⁴¹Pu,
●—● : TIMS, ▲—▲ : ETOX

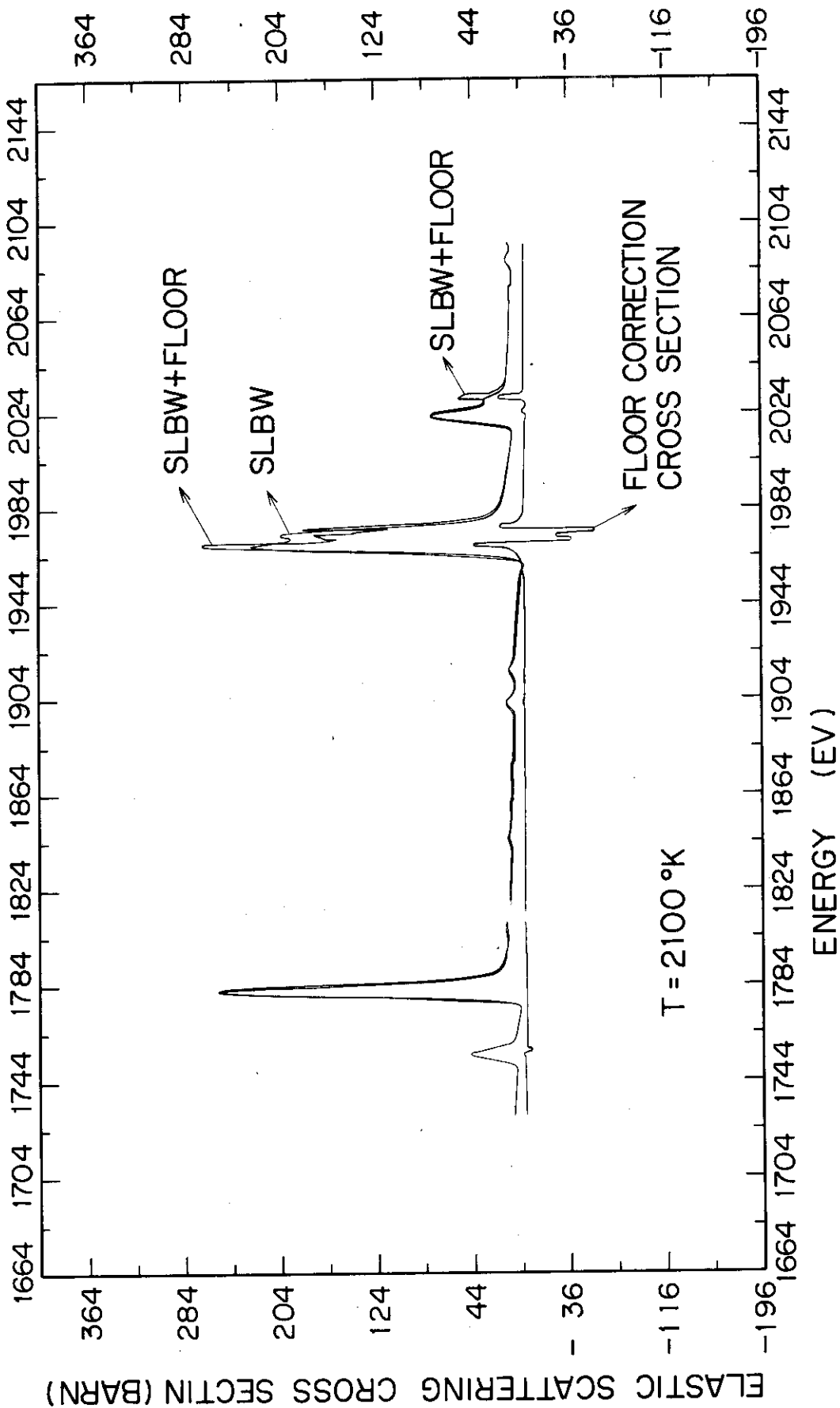


Fig. 6 Unreasonable Doppler-broadened cross sections caused by large values of floor correction cross sections

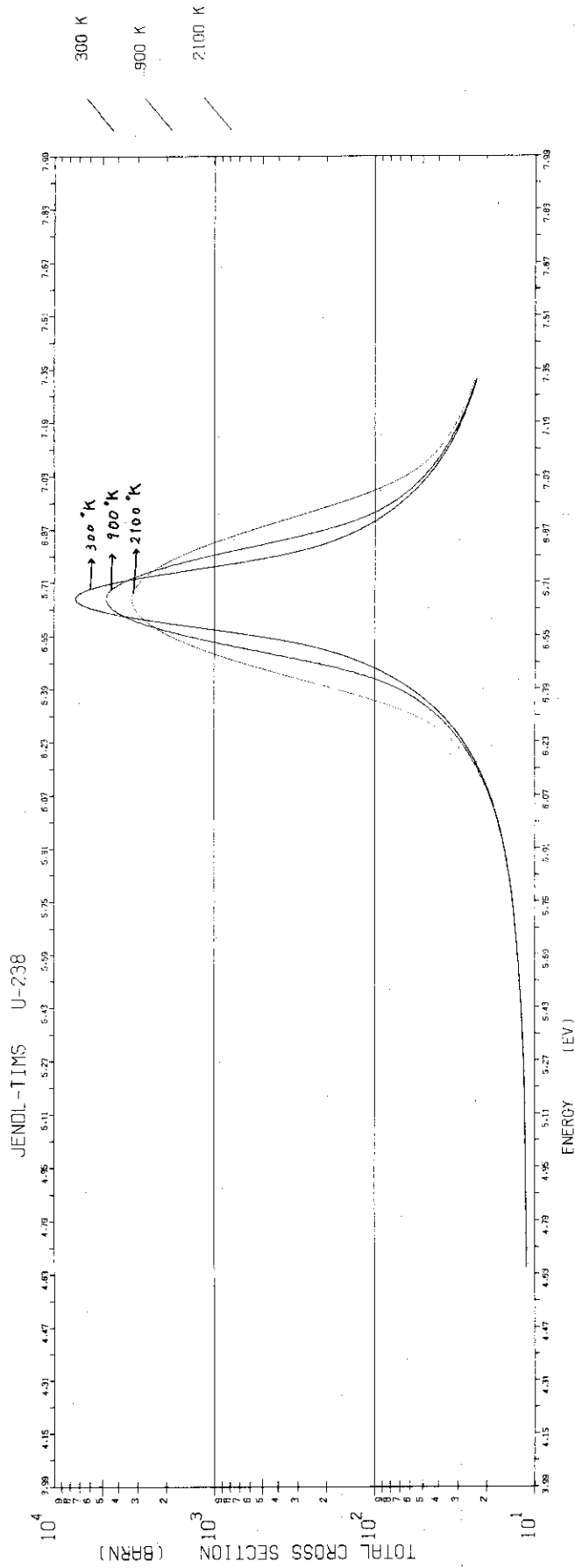


Fig. 7 Doppler broadened cross sections of ²³⁸U in the energy range from 4.65 to 7.35 eV

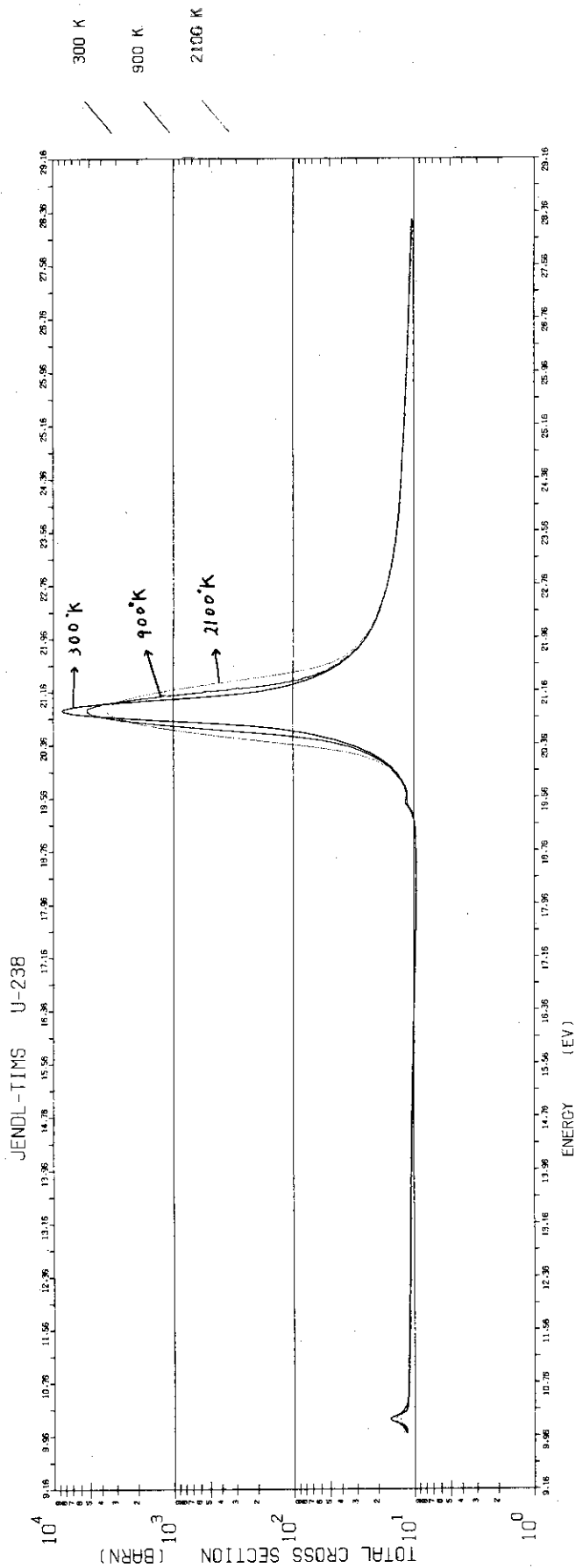


Fig. 8 Doppler broadened cross sections of ^{238}U in the energy range from 9.9 to 28 eV

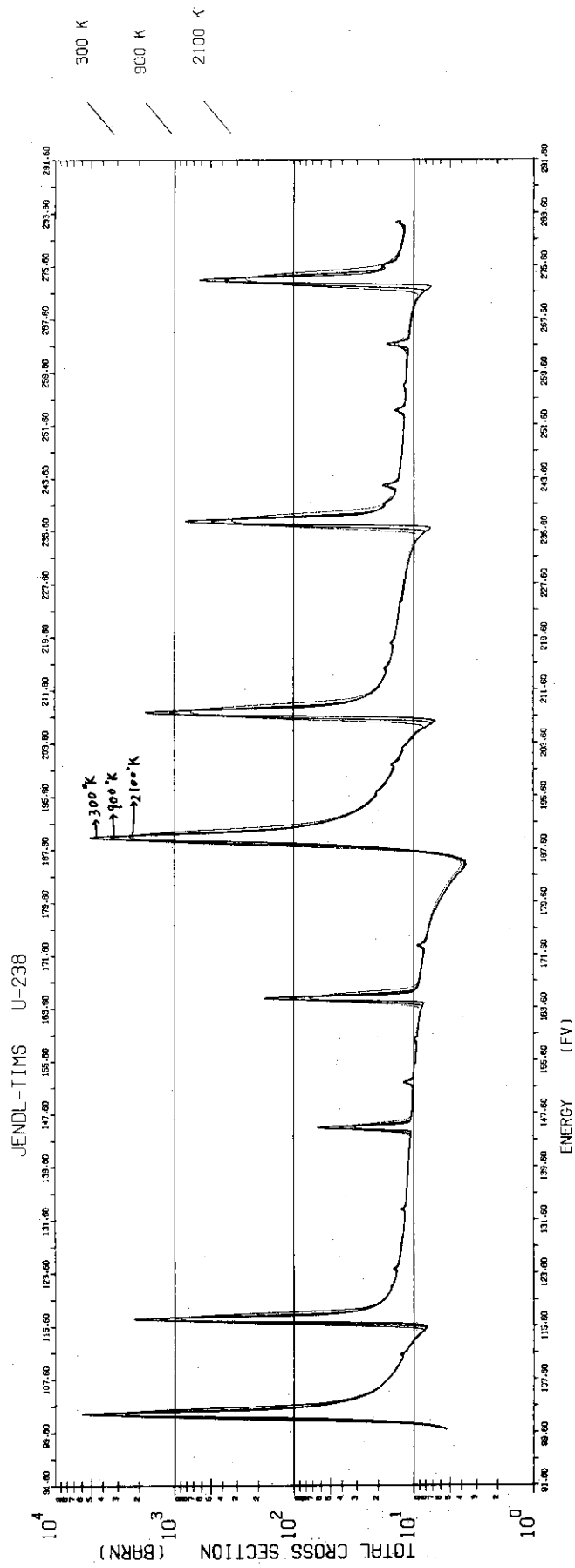


Fig. 9 Doppler broadened cross sections of ^{238}U in the energy range from 99.6 to 280 eV

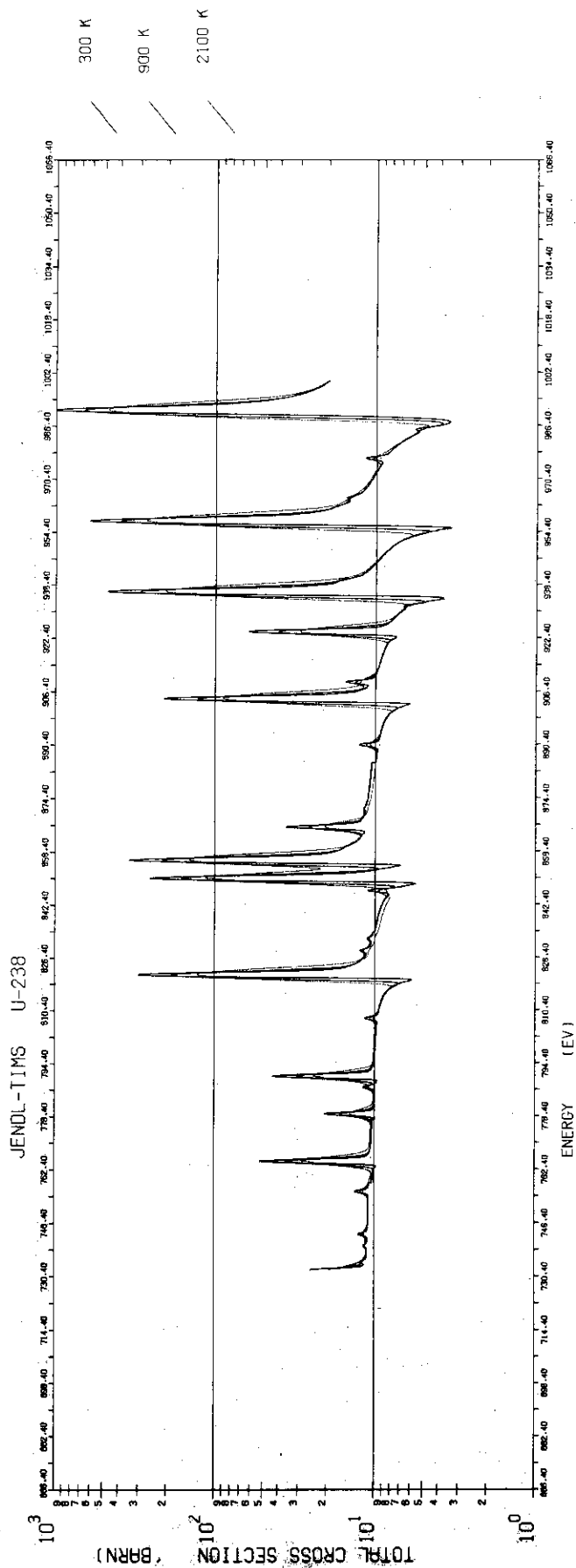


Fig. 10 Doppler broadened cross sections of ^{238}U in the energy range from 730 to 1000 eV

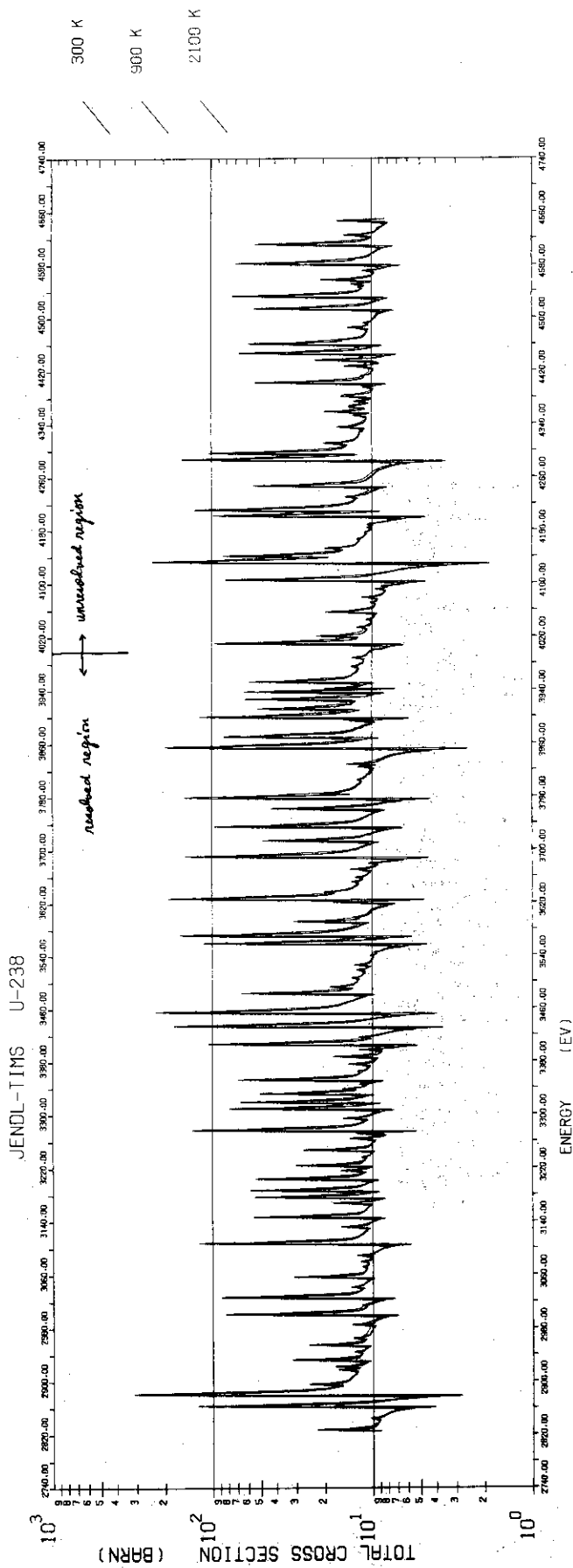


Fig. 11 Doppler broadened cross sections of ^{238}U in the energy range from 2820 to 4650 eV

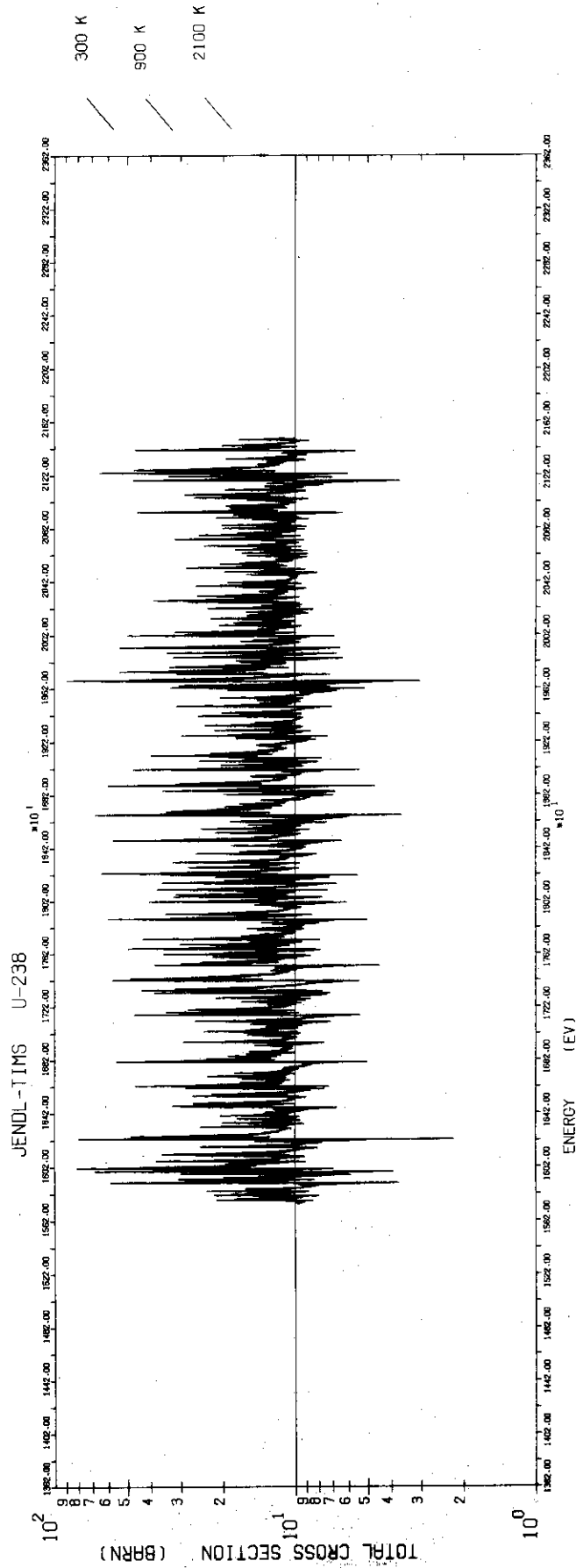


Fig. 12 Doppler broadened cross sections of ²³⁸U in the energy range from 15.62 to 21.5 keV

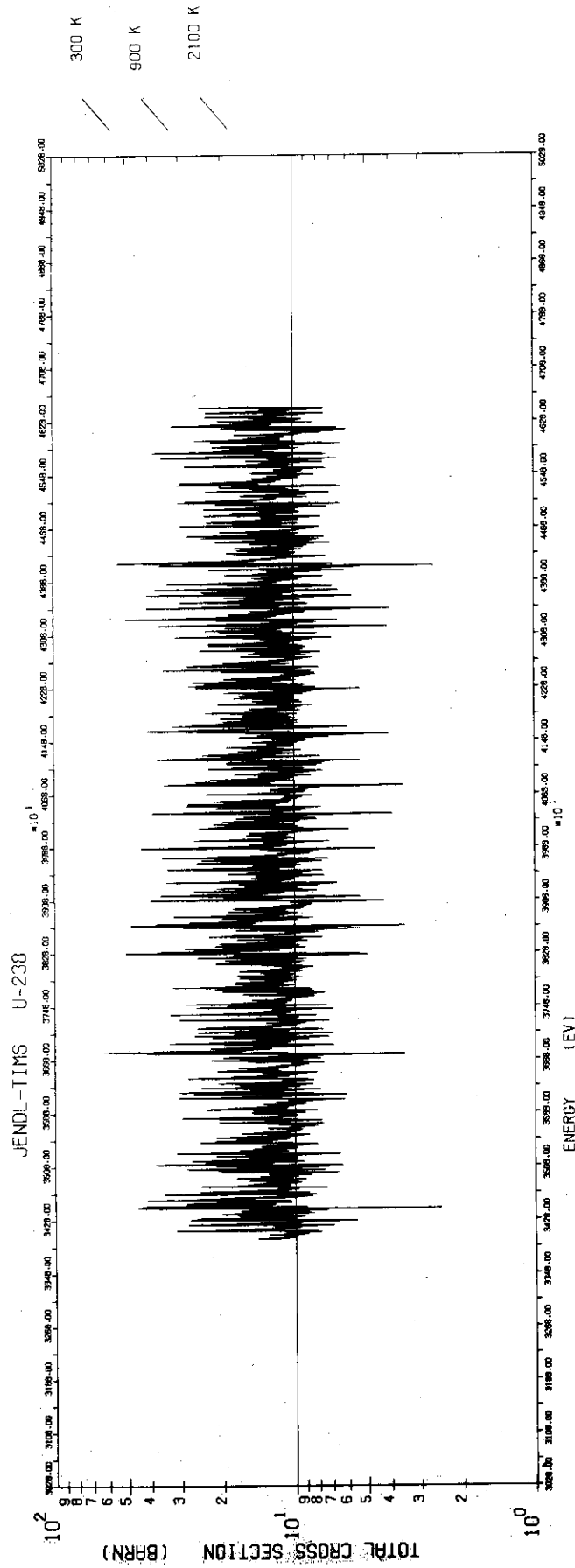


Fig. 13 Doppler broadened cross sections of ²³⁸U in the energy range from 34 to 46.5 keV

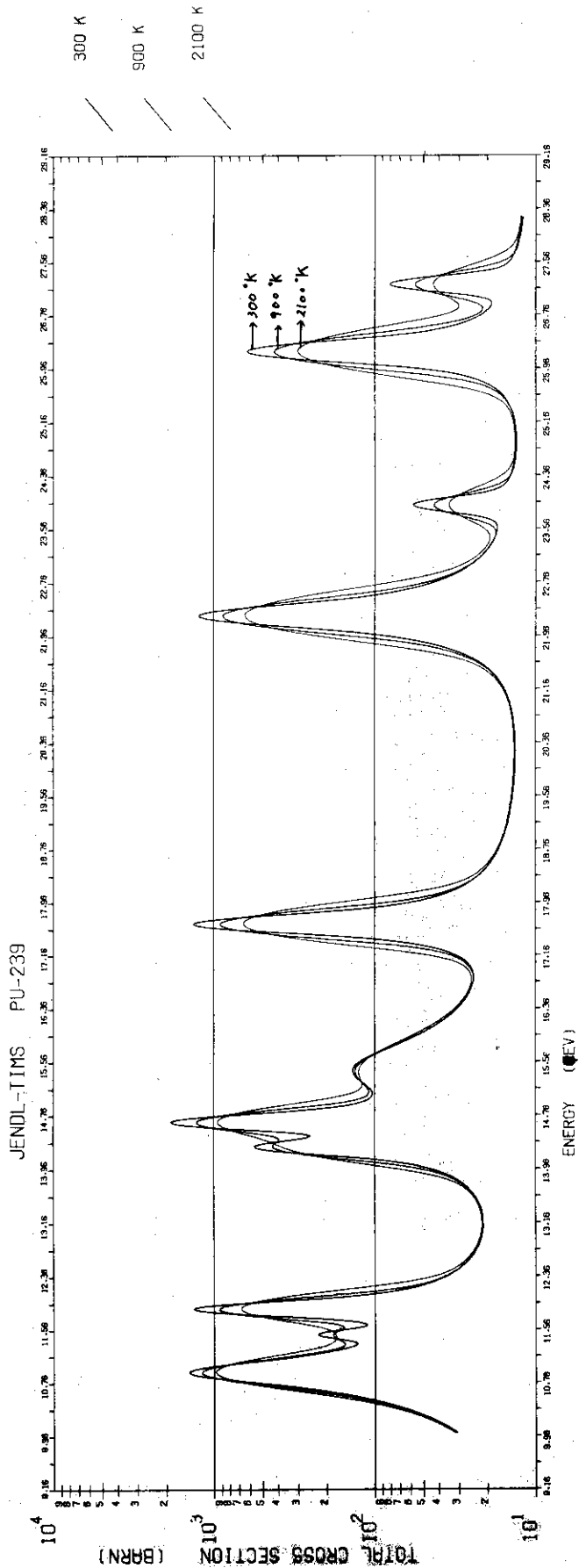


Fig. 14 Doppler broadened cross sections of ²³⁹Pu in the energy range from 9.96 to 27.8 eV

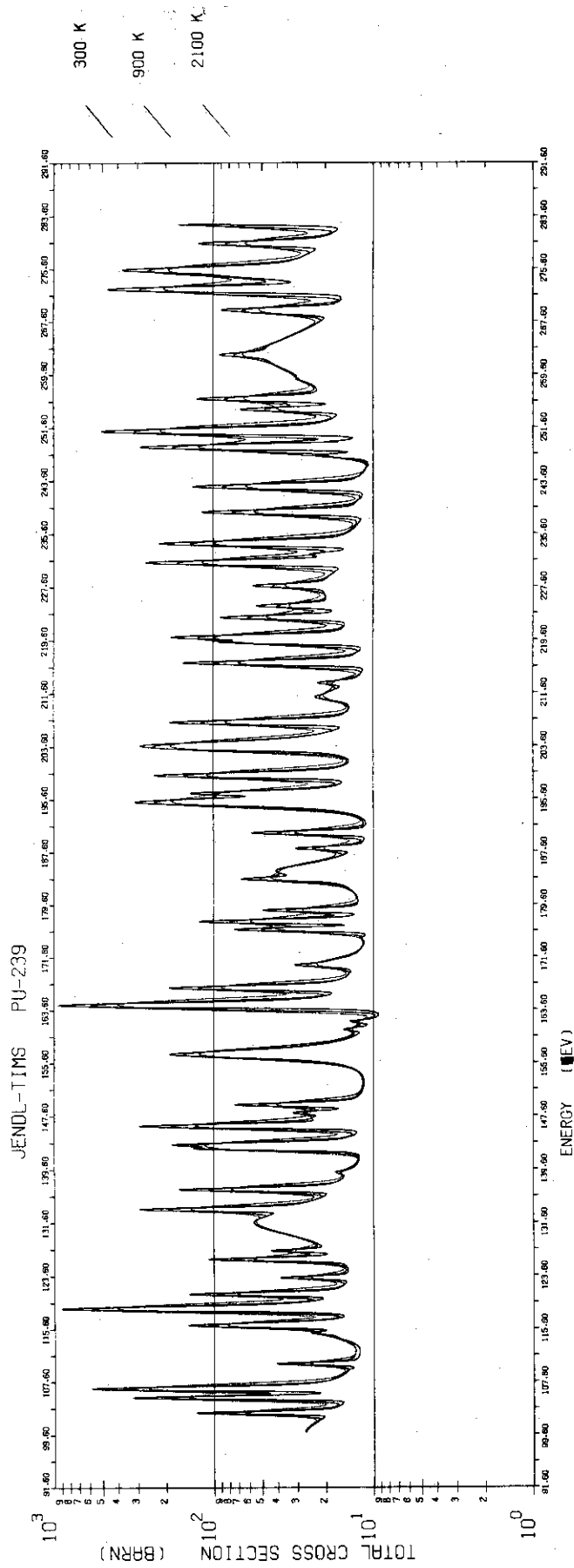


Fig. 15 Doppler broadened cross sections of ^{239}Pu in the energy range from 99.6 to 278 eV

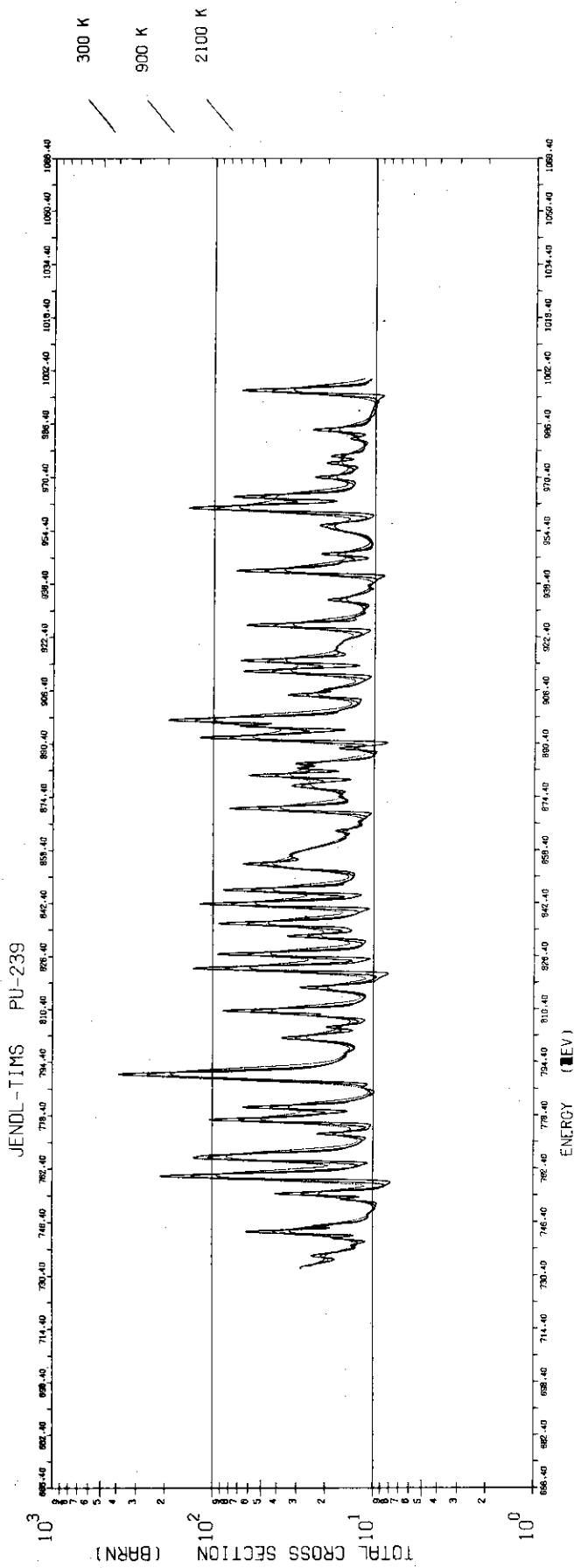


Fig. 16 Doppler broadened cross sections of ^{239}Pu in the energy range from 728 to 7000 eV

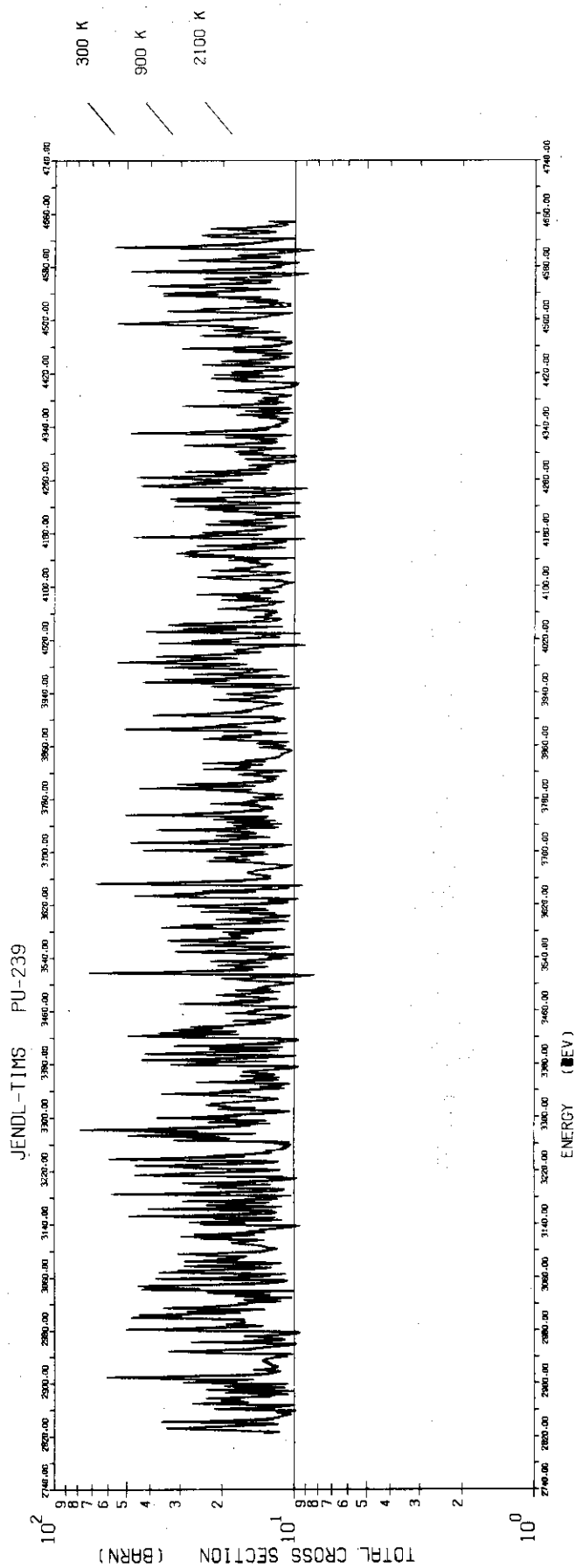


Fig. 17 Doppler broadened cross sections of ^{239}Pu in the energy range from 2780 to 4650 eV

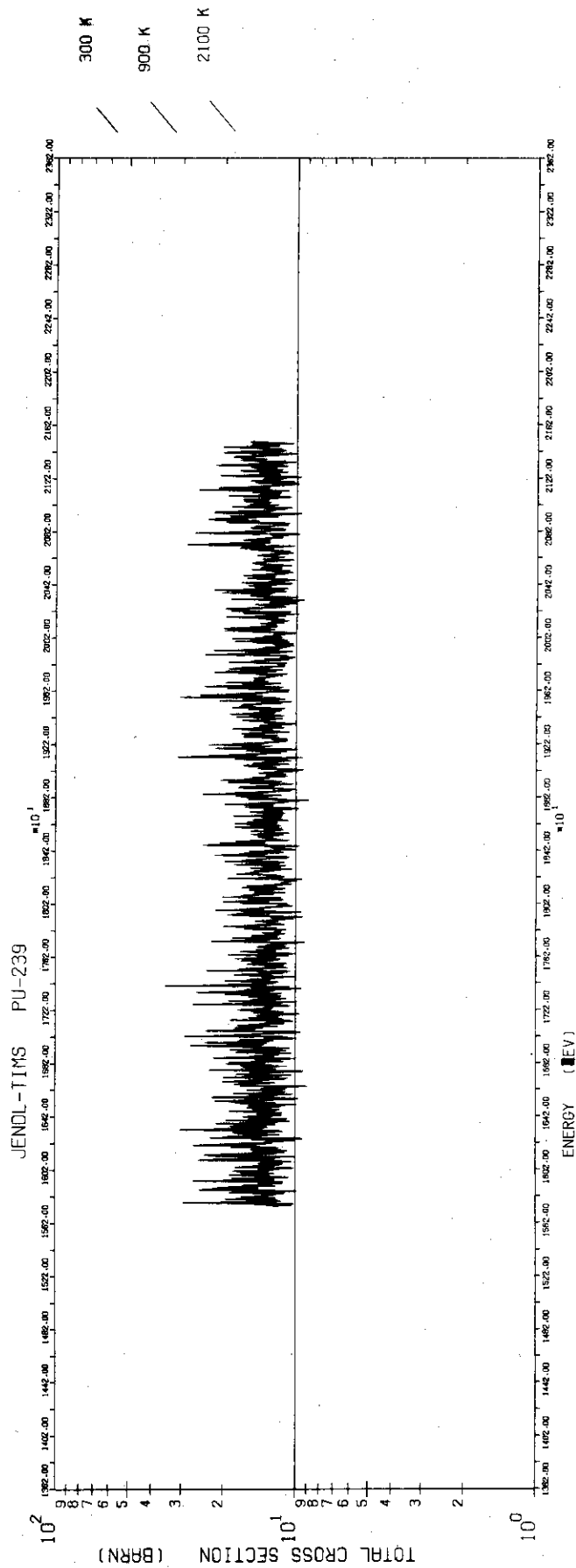


Fig. 18 Doppler broadened cross sections of ²³⁹Pu in the energy range from 15.62 to 21.5 keV

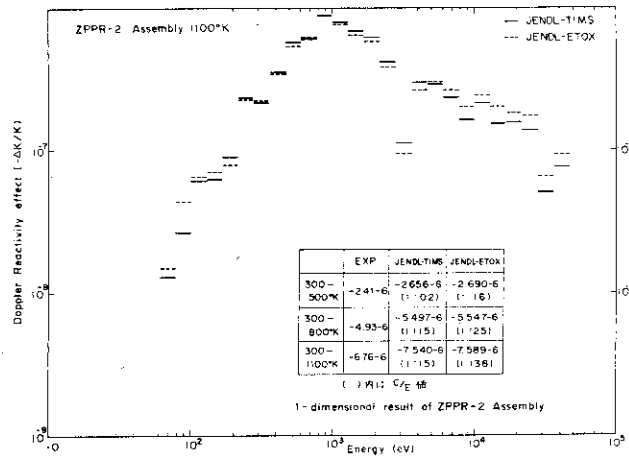


Fig. 19 Energy group-wise contribution of Doppler reactivity effect calculated by one-dimensional first order perturbation code for ZPPR assembly 2

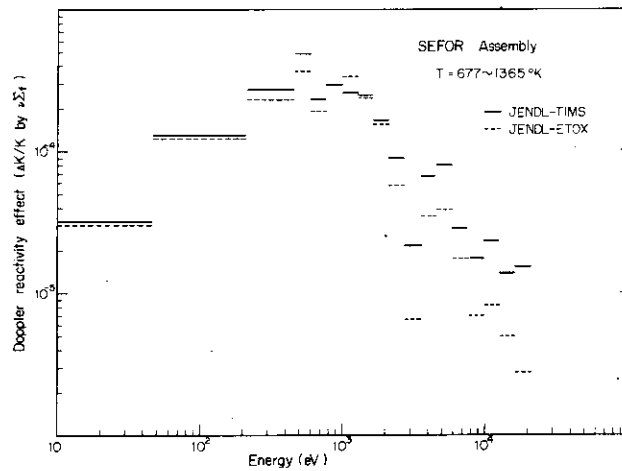


Fig. 20 Energy group-wise contribution of fission Doppler effect calculated by two-dimensional first order perturbation code for SEFOR assembly

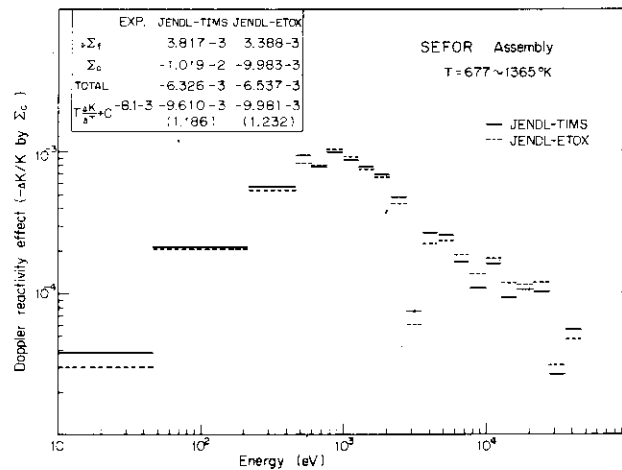


Fig. 21 Energy group-wise contribution of capture Doppler effect calculated by two-dimensional first order perturbation code for SEFOR assembly

APPENDIX : Tables of 70 Group Constants of ^{235}U , ^{238}U , ^{239}Pu , ^{240}Pu
and ^{241}Pu Produced by the Processing Code TIMS Using the Evaluated
Nuclear Data of JENDL-1

The results calculated with the TIMS code were arranged in the conventional form of the infinitely dilute cross sections and the resonance shielding factors. As already described in Chapter 2, the TIMS code can calculate the resonance shielding factors depending on the three variables; composition (σ_0), temperature (T) and mutual interference parameter (R), where R is defined by

$$R = \frac{^{238}\text{N}}{^{235}\text{N}}, \frac{^{238}\text{N}}{^{239}\text{N}} \text{ or } \frac{^{238}\text{N}}{^{240}\text{N}} .$$

In the present calculation, the two R-values were selected so as to cover the practical range of R depending on another composition variable σ_0 of the Bondarenko's type. These R-values are shown in Table A-1. The composition variable σ_0 considered for the calculation of effective cross sections without the mutual interference effect are shown in Table A-2. The considered temperatures were 300, 900 and 2100°K. The group constants depending on these variables were calculated with the group structure as shown in Table A-3. The group constants depending on the R-parameters are tabulated in Tables A-4.1 ~ 4.5, and those without considering the mutual interference effect are also tabulated in Tables A-5.1 ~ 5.5.

Table A-1. Values of atomic density ratios, R_1 and R_2 used for the consideration of the mutual interference effect of heavy nuclides with ^{238}U

σ_o (barns)	U-235		Pu-239		Pu-240	
	R_1	R_2	R_1	R_2	R_1	R_2
10000.	250.	500.	500.	1000.	200.	500.
1000.	25.	50.	50.	100.	20.	50.
100.	1.	5.	5.	10.	5.	15.
10.	0.2	0.6	1.	2.	—	—

Table A-2. Values of composition variable σ_o used for the calculation of the resonance shielding factors without the mutual interference effect

Nuclide	σ_o (barns)
U-235	0, 10, 100, 1000
U-238	0, 1, 10, 100, 1000
Pu-239	0, 10, 100, 1000
Pu-240	0, 100, 1000, 10000
Pu-241	0, 10, 100, 1000, 10000

Table A-3. 70-group structure

Group	Upper energy	Lower energy	Lethargy width
1	10.5 (MeV)	8.3	0.2351
2	8.3 (MeV)	6.5	0.2445
3	6.5 (MeV)	5.1	0.2426
4	5.1 (MeV)	4.0	0.2429
5	4.0 (MeV)	3.1	0.2549
6	3.1 (MeV)	2.5	0.2151
7	2.5 (MeV)	1.9	0.2744
8	1.9 (MeV)	1.4	0.3054
9	1.4 (MeV)	1.1	0.2412
10	1.1 (MeV)	0.8	0.3185
11	0.8 (MeV)	0.63	0.2389
12	0.63 (MeV)	0.50	0.2311
13	0.50 (MeV)	0.4	0.2231
14	0.4 (MeV)	0.31	0.2549
15	0.31 (MeV)	0.25	0.2151
16	0.25 (MeV)	0.2	0.2231
17	0.2 (MeV)	0.15	0.2877
18	0.15 (MeV)	0.12	0.2231
19	0.12 (MeV)	0.1	0.1823
20	100 (KeV)	77.3	0.2575
21	77.3 (KeV)	59.8	0.2567
22	59.8 (KeV)	46.5	0.2516
23	46.5 (KeV)	36.0	0.2559
24	36.0 (KeV)	27.8	0.2585
25	27.8 (KeV)	21.5	0.2570
26	21.5 (KeV)	16.6	0.2587
27	16.6 (KeV)	12.9	0.2522
28	12.9 (KeV)	10.0	0.2546
29	10.0 (KeV)	7.73	0.2575
30	7.73 (KeV)	5.98	0.2567
31	5.98 (KeV)	4.65	0.2516
32	4.65 (KeV)	3.60	0.2559
33	3.60 (KeV)	2.78	0.2585
34	2.78 (KeV)	2.15	0.2570
35	2.15 (KeV)	1.66	0.2587
36	1.66 (KeV)	1.29	0.2522
37	1.29 (KeV)	1.0	0.2546
38	1000 (eV)	773	0.2575
39	773 (eV)	598	0.2567
40	598 (eV)	465	0.2516
41	465 (eV)	360	0.2559
42	360 (eV)	278	0.2585
43	278 (eV)	215	0.2570
44	215 (eV)	166	0.2587
45	166 (eV)	129	0.2522
46	129 (eV)	100	0.2546
47	100 (eV)	77.3	0.2575

Table A-3. (Continued)

Group	Upper energy	Lower energy	Lethargy width
48	77.3 (eV)	59.8	0.2567
49	59.8 (eV)	46.5	0.2516
50	46.5 (eV)	36.0	0.2559
51	36.0 (eV)	27.8	0.2585
52	27.8 (eV)	21.5	0.2570
53	21.5 (eV)	16.6	0.2587
54	16.6 (eV)	12.9	0.2522
55	12.9 (eV)	10.0	0.2546
56	10.0 (eV)	7.73	0.2575
57	7.73 (eV)	5.98	0.2567
58	5.98 (eV)	4.65	0.2516
59	4.65 (eV)	3.60	0.2559
60	3.60 (eV)	2.78	0.2585
61	2.78 (eV)	2.15	0.2570
62	2.15 (eV)	1.66	0.2587
63	1.66 (eV)	1.29	0.2522
64	1.29 (eV)	1.0	0.2546
65	1.0 (eV)	0.773	0.2575
66	0.773(eV)	0.598	0.2567
67	0.598(eV)	0.465	0.2516
68	0.465(eV)	0.360	0.2559
69	0.360(eV)	0.278	0.2585
70	0.278(eV)	0.215	0.2570

Table A-4.1 INFINITE DILUTION CROSS SECTION CODE NO = 925

Table with 10 columns: GROUP, TOTAL, FISSION, NU, CAPTURE, INELASTIC, ELASTIC, MU, ELAS, REMOVAL. It contains a detailed list of nuclear cross-section data for various isotopes and energy levels.

Table A-4.2 SELF -SHIELDING FACTOR TABLES CODE NO = 925

Table with 11 columns: GROUP, T(K), FF1 (10., 100., 1000.), FF2 (10., 100., 1000.), FC1 (10., 100., 1000.), FC2 (10., 100., 1000.). It provides self-shielding factors for different temperature groups and energy levels.

Table A-4.3.1 INFINITE DILUTION CROSS SECTION CODE NO = 949

PU-239,1 PAGE 1

Table with columns: GROUP, TOTAL, FISSION, NU, CAPTURE, INELASTIC, ELASTIC, MU, ELAS, REMOVAL. Contains 40 rows of numerical data.

Table A-4.3.2

SELF -SHIELDING FACTOR TABLES CODE NO = 949

Table with columns: GROUP, T(K), FF1, FF2, FC1, FC2. Each of the four factor columns has sub-columns for values at 10, 100, and 1000. Contains 40 rows of numerical data.

Table A-4.3.2 (continued)

Table with columns: GROUP, T(K), FE1 (10.0, 100.0, 1000.0), FE2 (10.0, 100.0, 1000.0), FT1 (10.0, 100.0, 1000.0), FT2 (10.0, 100.0, 1000.0). Rows are numbered 61 to 70.

Table with columns: GROUP, T(K), FR1 (10.0, 100.0, 1000.0), FR2 (10.0, 100.0, 1000.0), GROUP, T(K), FR1 (10.0, 100.0, 1000.0), FR2 (10.0, 100.0, 1000.0). Rows are numbered 26 to 70.

Table A-4.4.2 (continued)

Table with columns for GROUP T(K), FE1 (100, 1000, 10000), FE2 (100, 1000, 10000), FT1 (100, 1000, 10000), and FT2 (100, 1000, 10000). Rows represent different temperature groups (50-70) and their respective data points.

Large multi-column table containing data for groups 23 through 70. Each group has multiple rows for temperatures 300, 900, and 2100 K. Columns include parameters like FR1, FR2, and various numerical values.

Table A-4.5.1

INFINITE DILUTION CROSS SECTION CODE NO = 941

PU-241.1 PAGE 1

Table with 10 columns: GROUP, TOTAL, FISSION, NU, CAPTURE, INELASTIC, ELASTIC, MU, ELAS, REMOVAL. It contains a list of nuclear data points for various isotopes and reactions.

Table A-4.5.2

SELF -SHIELDING FACTOR TABLES CODE NO = 941

A large multi-column table containing self-shielding factor data. Columns are grouped under FF, FC, FE, and FT, each with sub-columns for different energy levels (10, 100, 1000, 10000). Rows correspond to different groups and temperatures (300, 900, 2100).

Table A-4.4

SELF-IRRADIATION FACTOR TABLES CODE NO = 940

PU-240 PAGE 1

Table with columns: GROUP, T(K), FF (0, 100, 1000, 10000), FC (0, 100, 1000, 10000), FE (0, 100, 1000, 10000), FT (0, 100, 1000, 10000). Rows range from 23 to 59 and 300 to 2100 K.

Table A-5.5 (continued)

Table with columns: GROUP, T(K), O., 10, FR (100, 1000, 10000), and corresponding values for groups 26 through 70. Each group entry includes three rows for different temperatures (300, 900, 2100 K).